J. Nannoplankton Res. **37** (2–3), 2017, pp.113–144 © 2017 International Nannoplankton Association
ISSN 1210-8049 Printed by The Sheridan Press, USA

Upper Miocene-Lower Pliocene taxonomy and stratigraphy in the circum North Atlantic Basin: radiation and extinction of Amauroliths, Ceratoliths and the *D. quinqueramus* lineage

Stacie Blair*
Blair Biostratigraphy, Cypress, TX 77429 USA; *stacie.blair81@gmail.com

Jim Bergen
Paleo at the Hill Country, Brenham, TX 77833 USA; jbnanno@att.net

Eric de Kaenel
DPR, Chemin sous la Roche 4b, 1185 Mont-sur-Rolle, Switzerland; edekaenel@bluewin.ch

Emily Browning
BP America Inc., 200 Westlake Park Blvd, Houston, TX 77079 USA; Emily.Browning@bp.com

Todd Boesiger
ALS Global, Lincoln, NE 68506 USA; tboesig@gmail.com

Manuscript received 12th September, 2016; revised manuscript accepted 24th May, 2017

Abstract Three Neogene nannofossil lineages evolved rapidly in the Late Miocene to Early Pliocene: the Amauroliths, the Ceratoliths and the *Discoaster quinqueramus* lineage. The evolution of these lineages has been extensively studied within the petroleum industry, in particular BP America Inc. and its heritage companies, due to their considerable utility in the deep-water Gulf of Mexico. This study presents their biostratigraphic usage and taxonomic concepts for the Upper Miocene-Lower Pliocene interval (NN8-NN14). They are further defined utilizing astronomically "tuned" sediments from Ocean Drilling Program Leg 154 (western equatorial Atlantic), yielding 42 primary calibrated nannfossil events. Based on these results, we divide Zone NN12 (Martini, 1971) into two new Subzones (NN12a & b) and emend its top and base. Additionally, the taxonomy and stratigraphic distribution of Amauroliths, Ceratoliths, and the *D. quinqueramus* lineage are clarified. Three new Amaurolith and Ceratolith taxa are described, *A. brevigracilis, C. apiculus* and *C. cornulum* as well as eleven new species of *Discoaster*: *D. abrachiatus, D. astellaris, D. compactus, D. consutus, D. explicatus, D. gemmulatus, D. hexaramus, D. newellii, D. prolixus, D. tetracladus* and *D. vinsonii*. In addition, several taxa are formally emended.

Keywords *Ceratolithus, Amaurolithus, Discoaster,* nannofossils, Pliocene, Miocene, taxonomy, Gulf of Mexico, ODP Leg 154, biostratigraphy

1. Introduction

In the last few decades, microfossils have become an integral tool in subsurface petroleum exploration. Frontier exploration into stratigraphically- and structurally-complex fields, and the need for finer correlations in reservoir intervals, necessitated improvement of nannofossil biostratigraphies. As such, many petroleum companies built upon the standard global zonations (Martini, 1971; Okada & Bukry, 1980) and developed their own "in-house" biostratigraphic charts. These company-derived biostratigraphic frameworks are utilized in all phases of a well "life cycle" from planning/exploration to development/production.

This paper details the development of British Petroleum (BP) biostratigraphy in the deep-water Gulf of Mexico (GoM), in particular, focusing on the interval following economic recovery of the oil industry during the 1990s. In this upturn, three companies were merged: BP, Amoco, and Arco Vastar. This merger challenged staff to integrate three independently-derived microfossil frameworks from research developed over the past four decades; however, it became apparent that these three distinct frameworks also had considerable taxonomic discrepancies amongst them. Reanalysis of well cuttings, taxa documentation, and staunch communication between specialists both inside and outside of BP allowed for conversion of these three independent frameworks into one integrated BP GoM Cenozoic framework with improved definition and biostratigraphic resolution. For nannofossils, this resulted in the recognition of over 100 new taxa and strict taxonomic refinement for hundreds of documented species. Following this initial phase, advances in time-scale construction (*i.e.,* cyclostratigraphy and stage boundary stratotypes) prompted an in-house research program in 2002, its purpose to

ground the integrated BP GoM Cenozoic framework to an "astronomically-tuned" age model utilizing core material from Ocean Drilling Program (ODP) Leg 154, Ceará Rise. By 2013, this research spanned the middle Early Oligocene (30.679Ma) through Early Pleistocene (1.595Ma) and included detailed work on the Miocene/Pliocene boundary. This final integration of the BP GoM Cenozoic Framework and ODP Leg 154 research is to be collectively published in a separate paper, "BP Gulf of Mexico Neogene Astronomically-tuned Time Scale" (GNATTS; Bergen *et al*., in prep).

This is one of five taxonomic papers presented in this volume by the BP GoM team's research. Taxa presented and discussed in these papers largely comprise the nannofossil framework for the GNATTS. The papers are organized by taxonomic groups in approximate chronostratigraphic order: *Sphenolithus* (Bergen *et al*., 2017), *Helicosphaera* and placoliths (Boesiger *et al*., 2017), latest Oligocene-Middle Miocene *Discoaster* (de Kaenel *et al*., 2017), Middle-Upper Miocene *Discoaster* (Browning *et al*., 2017; some Pliocene forms included), and uppermost Miocene-Pliocene *Discoaster*, *Amaurolithus*, and *Ceratolithus* (herein). This paper focuses on refining the taxonomy and stratigraphy of the aforementioned nannofossil taxa and events associated with major radiations and extinctions across to the Miocene/Pliocene boundary from roughly 11.0–4.5Ma.

There are at least three major radiation and extinction events observed in the Ceratoliths, Amauroliths and the *Discoaster quinqueramus* lineage across the Miocene/Pliocene transition. Some of these events have been long-used in the standard global zonations of Martini (1971) and Okada & Bukry (1980). This study expands upon the three groups' biostratigraphic utility by providing 42 primary calibrated biostratigraphic events, 14 new taxa descriptions and several emendations.

2. Materials and Methods

The materials used for this study include core and well cuttings from three localities (Figure 1): 1) the Columbia Basin, western Caribbean Sea (Deep Sea Drilling Project [DSDP] Leg 68, Site 502); 2) Ceará Rise, western Equatorial Atlantic Ocean (ODP Leg 154, Site 926); and 3) Gulf of Mexico. Core material from ODP Leg 154 was sampled at ~21-ky resolution to astronomically "tune" the BP biostratigraphic framework. Details of the Leg 154 sampling program and calibration is provided in de Kaenel *et al.* (2017, this volume) and Bergen *et al.* (in prep). Nannofossil event ages detailed in this study are derived primarily from that research. Well-preserved Upper Miocene-Lower Pliocene assemblages recovered by centrifuging of core material from DSDP Site 502 proved especially helpful in the documentation of nannofossil taxa and provided much of the holotype material. The GoM samples are cuttings from petroleum exploration wells that contained well-preserved assemblages used in illustrations and holotypes. Holotype samples and slides are housed in the Natural History Museum in Basel, Switzerland.

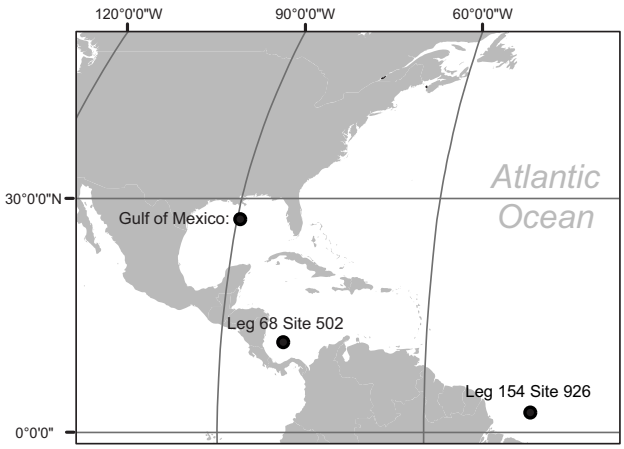

Figure 1: Map showing the locations of sample materials utilized and discussed in this study: the Ceará Rise (ODP Leg 154, Site 926), the Columbia Basin, western Caribbean Sea (DSDP Leg 68, Site 502) and the Gulf of Mexico

All biostratigraphic event calibrations are based on 15 years of analyses of the ODP Leg 154 materials; many of these events are included in the BP GNATTS framework (Bergen *et al.*, in prep). Events were cross-checked by multiple nannopaleontologists and taxonomic concepts were synchronized between Leg 154 and the GoM. The GNATTS scheme was also correlated to the standard zonations of Martini (1971) and Okada & Bukry (1980) with some emendations. In this paper, all taxa ranges are expressed in NN Zones (Martini, 1971) with ages primarily obtained by our study of Leg 154 materials. The abbreviations HO (highest occurrence), HRO (highest regular occurrence), LO (lowest occurrence) and LRO (lowest regular occurrence) are utilized in the following text and Table 1 to describe biostratigraphic events.

The objective of this paper is to clarify taxonomic concepts and present the GoM stratigraphy developed over the past five decades from the three BP heritage companies. Where pertinent, only minor, key comparisons to other published stratigraphies of the GoM Basin and research on ODP Leg 154 are given. The geologic ages derived from ODP Leg 154 samples are maintained at three decimal precision through the manuscript for consistency; errors given on ages reflect the difference in age for the next sample analyzed upwards or downwards in the composite section. Links to supplementary materials are provided with the digital publication located on the *Journal's* website (http://ina.tmsoc.org/JNR/JNRcontents.htm) and include biometrics. Stratigraphic range charts and nannofossil abundance data are available on the web database PANGAEA (www.pangaea.de). Only those taxonomic references not documented in Perch-Nielsen (1985) are included in the reference section.

3. Biostratigraphy

The Miocene-Pliocene boundary falls within nannofossil Zone NN12 (Martini, 1971) and is equivalent to Subzones

Taxon	Event	Zone (Martini, 1971)	Age (Ma)	Error$_1$ (Ma)	Hole-Core-Sec. cm-cm	Depth (rmcd)$_2$
A. delicatus	HO	NN15	3.933	0.024	926C-12H-3, 145-146	122.06
A. delicatus	HRO	NN15	4.379	0.025	926B-14H-1, 45-46	137.36
A. tricorniculatus	HO	**top NN14**	4.445	0.017	926B-14H-2, 50-51	138.91
A. tricorniculatus	HRO	NN14	4.596	0.019	926C-14H-2, 120-121	142.89
C. armatus	HO	NN14	4.666	0.022	926B-14H-6, 30-31	144.71
C. acutus	HO	NN14	4.812	0.008	926B-15H-1, 120-122	148.57
C. cristatus	LO	**top NN12b**	5.059	0.017	926B-15H-6, 70-71	155.57
C. atlanticus	HO	NN12b	5.147	0.013	926A-16H-2, 105-106	157.51
C. apiculus	HO	NN12b	5.172	0.025	926A-16H-3, 15-16	158.11
C. cornulum	LO	NN12b	5.310	0.010	926A-16H-5, 25-26	161.21
C. acutus	LO	**top NN12a**	5.340	0.014	926A-16H-5, 84-85	161.80
D. quintatus	HO	NN12a	5.365	0.003	926A-16H-5, 135-136	162.31
C. apiculus	LO	NN12a	5.372	0.017	926A-16H-6, 8-9	162.54
C. atlanticus	LO	NN12a	5.389	0.027	926A-16H-6, 45-46	162.91
D. quinqueramus	HO	**top NN11b**	5.440	0.024	926C-16H-6, 145-146	163.91
D. berggrenii	HO	NN11b	5.772	0.013	926B-17H-2, 64-65	171.11
D. quinqueramus (>15)	HRO	NN11b	5.932	0.023	926B-17H-4, 127-128	174.74
D. vinsonii	HO	NN11b	6.120	0.024	926C-17H-5, 28-29	178.51
D. compactus	HO	NN11b	6.233	0.021	926C-17H-6, 64-65	180.37
D. compactus	HRO	NN11b	6.325	0.020	926B-18H-2, 148-149	182.02
D. newellii	HRO/INC	NN11b	6.423$_3$	0.018	926B-18H-4, 31-32	183.85
A. amplificus	INC	NN11b	6.445	0.022	926B-18H-4, 73-74	184.27
D. vinsonii	HFO/INC	NN11b	6.638	0.017	926B-18H-6, 106-107	187.60
D. abrachiatus	HO	NN11b	6.710	0.026	926C-18H-6, 10-11	189.09
D. compactus	INC	NN11b	6.710	0.026	926C-18H-6, 10-11	189.09
D. bergenii	HO	NN11b	6.801	0.022	926C-18H-7, 16-17	190.65
A. amplificus	LO	NN11b	6.930	0.020	926B-19H-2, 148-149	192.82
D. compactus	HFO/HOAc	NN11b	7.065	0.021	926B-19H-4, 67-68	195.01
D. abrachiatus	INC	NN11b	7.305	0.020	926B-19H-6, 40-41	197.74
A. delicatus	LO	NN11b	7.332	0.015	926B-19H-6, 85-86	198.19
D. hexaramus	HO	NN11b	7.438	0.017	926A-20H-3, 84-85	200.82
D. abrachiatus	DEC	NN11b	7.542	0.017	926A-20H-4, 84-85	202.32
A. primus	LO	**top NN11a**	7.559	0.007	926A-20H-4, 105-106	202.53
C. mexicanus	HO	NN11a	7.566	0.007	926B-20H-2, 22-23	202.41
D. astellaris	HO	NN11a	7.912	0.022	926B-20H-5, 136-137	208.05
D. gemmulatus	HO	NN11a	8.025	0.012	926B-21H-2, 64-65	211.83
C. mexicanus	LO	NN11a	8.204	0.025	926B-21H-5, 6-7	215.75
D. newellii	LO	NN11a	8.229	0.032	926B-21H-5, 61-62	216.30
D. vinsonii	LO	NN11a	8.292	0.001	926B-21H-6, 32-33	217.51
D. quinqueramus	LO	**top NN10**	8.317	0.027	926C-22H-1, 128-129	218.36
D. berggrenii	LO	NN10	8.317	0.027	926C-22H-1, 128-129	218.36
D. bellus	HCO/HO	NN10	8.344	0.027	926C-22H-2, 27-28	218.85

Table 1: Main events for the *D. quinqueramus,* Ceratolith and Amaurolith lineages as observed in Leg 154 and Gulf of Mexico. $_1$error in age of next sample. $_2$revised meters composite depth. $_3$proxy: increase in total abundance. HOAc=highest occurrence of acme. HFO=highest frequent occurrence

CN10a-b of Okada & Bukry (1980). Zone NN12 is defined at its base by the HO of *Discoaster quinqueramus* and its top by the LO of *Ceratolithus rugosus*. These two nannofossil events bracket the Miocene/Pliocene boundary in both the NN and CN zonations. The HO of *Ceratolithus acutus* and the LO of *C. rugosus* are intra-NN12 events used to define the top of Subzone CN10b. The CN10a/CN10b zonal boundary is defined both by the LO of *C. acutus* and HO of *Triquetrorhabdulus rugosus*. This study fromally divides Zone NN12 into two Subzones to coincide with Subzones CN10a/CN10b and provides revised taxonomic definition of zonal markers as well as abandonment of multiple criteria for zonal boundaries.

3.1 NN12a – *Ceratolithus atlanticus* Subzone

Definition: Interval from the top of *Discoaster quinqueramus* to the base of *Ceratolithus acutus.*

Authors: Blair & Bergen, this paper.

Reference locality: ODP Leg 154, 163.91 to 161.80 rmcd (revised measured composite depth) from Sample 926C-16H-6, 145–146cm to Sample 926A-16H-5, 84–85cm.

Discussion: The base of Subzone NN12a, the HO of *D. quinqueramus*, is dated at 5.440Ma (+/-0.024) in our Leg 154 research. Care must be taken to differentiate

Discoaster quinqueramus from *Discoaster quintatus* (see discussion in Systematic Paleontology). The HO of *D. quintatus* is dated at 5.365Ma (+/-0.003) and occurs within Subzone NN12a. The LO of *Ceratolithus acutus*, dated at 5.340Ma (+/-0.014) in our Leg 154 research, defines the top of Subzone NN12a. The LO of *Ceratolithus atlanticus* (5.389Ma; +/-0.027) may be used to further subdivide this short subzone commonly observed in deep-water GoM reference wells and our Leg 154 research (Table 1).

3.2 NN12b – *Ceratolithus acutus* Subzone

Definition: Interval from the base of *Ceratolithus acutus* to the base of *Ceratolithus cristatus.*

Authors: Blair & Bergen, this paper.

Reference locality: ODP Leg 154, 161.80 to 155.57 rmcd from Sample 926A-16H-5, 84–85cm to Sample 926B-15H-6, 70–71cm.

Discussion: The base of Subzone NN12b, the LO of *Ceratolithus acutus*, is dated at 5.340Ma (+/-0.014) in the ODP Leg 154 research. We emend here the base of Zone NN13 (Martini, 1971), substituting the LO of *Ceratolithus cristatus* for the LO of *Ceratolithus rugosus*, which is deemed unreliable due to its rarity in most marine sections, including the GoM. The LO of *Ceratolithus cristatus* is dated at 5.059Ma (+/-0.017) in our Leg 154 research. Other nannofossil events within this Subzone NN12b (= CN10b) common to deep-water GoM reference wells and our Leg 154 research (Table 1) in stratigraphic order are: LO *Ceratolithus cornulum* sp. nov. (5.310Ma; +/-0.010), HO *T. rugosus* (5.232Ma; +/-0.028), HO *C. apiculus* sp. nov. (5.172Ma; +/-0.025), and HO *C. atlanticus* (5.147Ma; +/-0.013).

4. Morphologic Variation and Radiation of the Amauroliths, Ceratoliths and the *D. quinqueramus* lineage

4.1 *Discoaster quinqueramus* lineage (See Figures 2–5)

Numerous studies have documented the striking morphological variability in the *D. quinqueramus* asterolith suite (Bukry, 1971; Theodoridis, 1984; Bergen, 1984; Perch-Nielsen, 1985; Knüttel *et al*., 1989; Raffi *et al*., 1998; Aubry, 2015). High sedimentation rates and overall good preservation in the Upper Miocene GoM prompted study and subdivision of the *D. quinqueramus* lineage morphotypes by numerous oil and gas companies prior to the turn of the century. These morphotypes provided better biostratigraphic resolution in these expanded sections than that of published nannofossil zonations; however, inter-company consensus was low due to independent taxonomic concepts and morphological definitions. The Gulf Coast Taxonomic Equivalency Project (GCTEP) was formed in the mid-1990s as a means to reveal and integrate taxonomic discrepancies of multiple Neogene nannofossil lineages as observed in various petroleum company research groups. One such group was the *D. quinqueramus* lineage. The GCTEP published an online diagram of the morphotypes utilized by some of the oil and gas companies (http://ina.tmsoc.org/Nannotax3/pages/GCEPquinq/Dquinq_lineage.html). At the time of this workshop, BP and its heritage companies did not release their species' concepts of the *D. quinqueramus* lineage. This paper discloses those species and morphotypic concepts developed by BP and its heritage companies as further defined by the ODP Leg 154 research.

Morphotypes of the *D. quinqueramus* lineage are subdivided based on their original descriptions, historical referencing and their BP GoM taxonomic definitions. Figure 2 gives an abbreviated depiction of morphological terms used here, modeled after Theodoridis (1984), Perch-Nielsen (1985), Young *et al*. (1997), and Aubry (2015). Primary morphological variation is observed in four key features (Figures 3–4): 1) free ray length to central area ratio; 2) presence or absence of a distal stellate stem and/or proximal knob; 3) size of the distal stellate stem relative to central area (*i.e*., knob to central area ratio); and 4) ray number. It has been shown there is stratigraphic utility in splitting taxa based on ray number (*e.g., D. brouweri, D. asymmetricus, D. tamalis,* and *D. triradiatus*); this is also true within the *D. quinqueramus* lineage.

Seventeen morphotypes within the *D. quinqueramus* lineage were identified; eleven are described in this study as new taxa (Figures 3–4; see also Systematic Paleontology). All have unique, many of them useful, biostratigraphic ranges. Preliminary biometric data for many of these forms can be accessed in the Supplementary Materials.

The divisions of the Upper Miocene are largely defined by the rapid radiation and extinction of this group of asteroliths (Figure 5). *Discoaster bellus,* the parent taxon of this lineage (Raffi *et al*., 1998; this study), is first observed in upper Zone NN8 (11.490Ma; 926A-26H-2, 4–6cm). *Discoaster gemmulatus* evolved from *D. bellus* in uppermost Zone NN8 (11.114Ma; 926A-25H-6, 70–72cm) and represents the first taxon in the *D. quinqueramus* lineage to develop a central knob. Rapid radiation of the group occurs in uppermost Zone NN10-lowermost Subzone NN11a with the inceptions of 11 taxa in the *D. quinqueramus* lineage evolving over a span of just ~350kyr. This interval represents major turnover as it also includes the extinctions

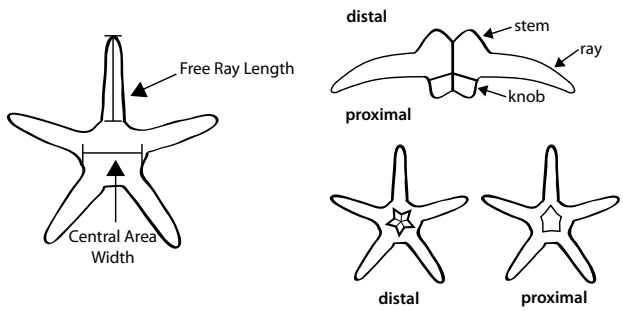

Figure 2: Diagram of morphologic terms utilized in this paper for the *D. quinqueramus* lineage [after Theodoridis (1984), Perch-Nielsen (1985), Young *et al*. (1997), and Aubry (2015)]

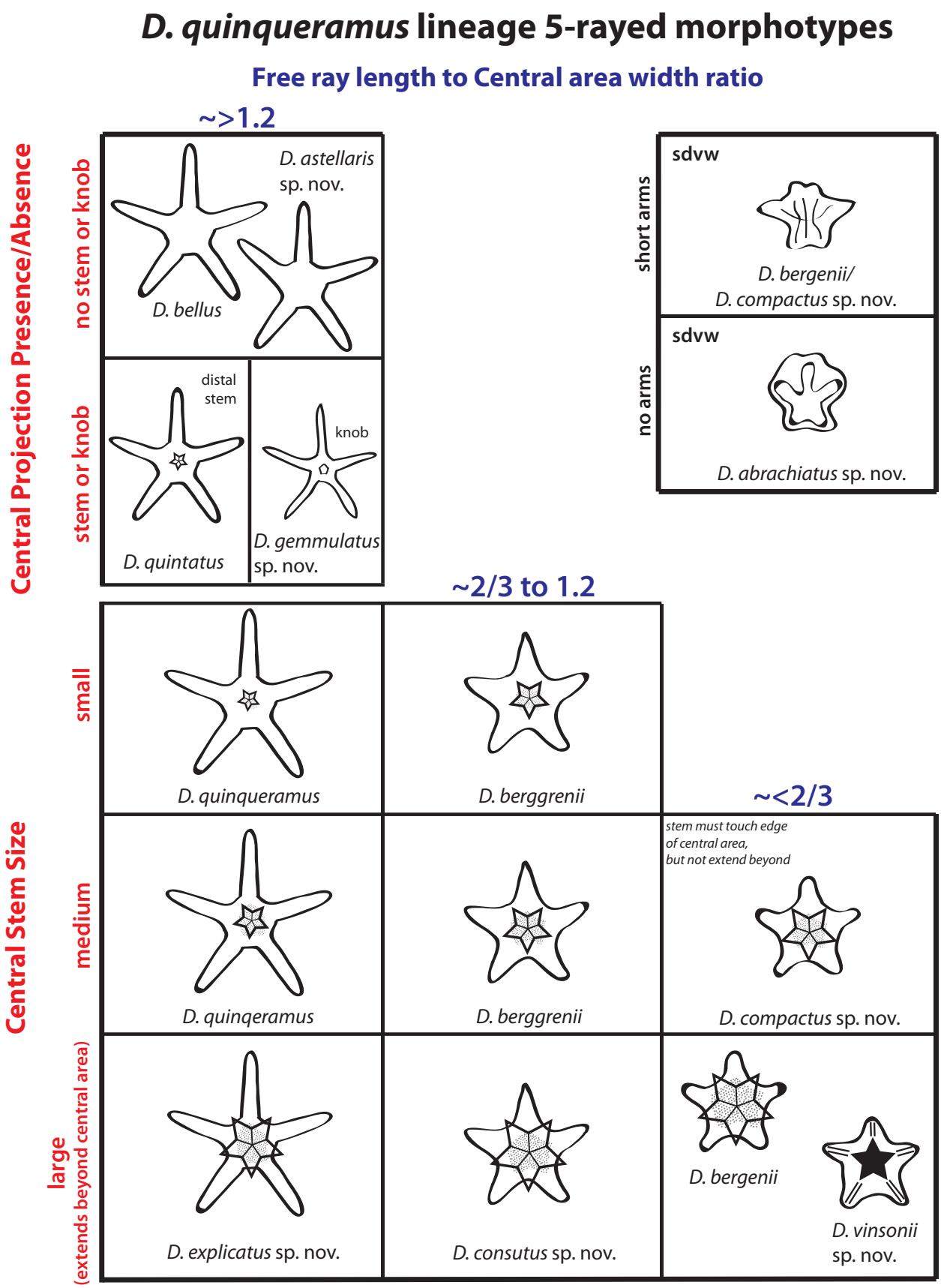

Figure 3: Morphotypic schematic of the five-rayed forms within the *D. quinqueramus* lineage largely subdivided based on free ray length to central area ratios and distal stem size. Sdvw=sideview

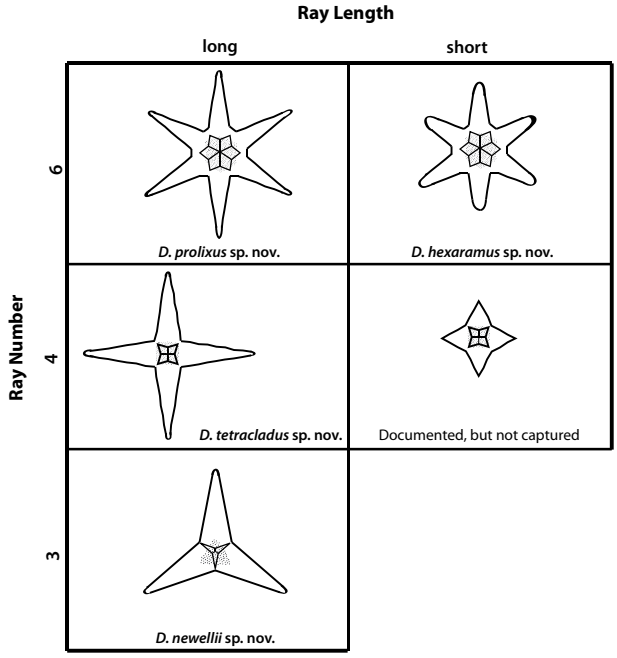

Figure 4: Morphotypic schematic of the three-, four-, and six-rayed forms of the *D. quinqueramus* lineage divided by ray length and number

of *D. bellus, D. astellaris*, and *D. gemmulatus*. During those 350kyr, morphological variation in ray number, ray length, central stem and knob size, and overall asterolith size distinguish the *D. quinqueramus* lineage. Eleven new species are described here: *D. abrachiatus, D. astellaris, D. compactus, D. consutus, D. explicatus, D. gemmulatus, D. hexaramus, D. newellii, D. prolixus, D. tetracladus* and *D. vinsonii*. These morphotypic splits yield taxa with extinctions and abundance fluctuations that provide substantial biostratigraphic resolution in Zones NN10-12; this includes roughly 23 major events and numerous minor events utilized by BP and its heritage companies (Table 1). At the group's termination, the end member taxon *D. quintatus* last occurs in basal Zone NN12a (5.365Ma; 926A-16H-5, 135–136cm), just ~32kyr below the Miocene/Pliocene boundary.

4.2 *Amaurolithus* (See Figure 6)

This genus is characterized as a horseshoe-shaped group that is non-birefrigent in cross-polarized light (XPL). There is considerable morphological variation including shape and size variability in the arch and horns, presence/absence and shape of an apical spine, as well as overall size differences. The genus ranges from the Upper Miocene to Lower Pliocene (base NN11b to upper NN15) spanning approximately 3.6 my based on our estimates from Leg 154. In the uppermost Tortonian-lowermost Messinian, rapid radiation of these taxa occurs immediately following the major turnover event of the *D. quinqueramus* lineage (Figure 6). The primary stratigraphic utility of the genus in the GoM is within the Lower Pliocene, as opposed to its importance in subdividing the upper Miocene Zone NN11 (CN9). A minimum of five Amaurolith inceptions occur over ~630kyr in Subzone NN11b. The lowest occurrence of *A. primus,* the parent taxon of the Amaurolith lineage, was observed at 7.559Ma (926A-20H-4, 105–106cm; +/-0.007Ma) and defines the base of Subzones NN11b (Martini) and CN9b (Okada & Bukry). *Amaurolithus delicatus*, the lineage upper endmember, last occurs in NN14 (3.933Ma; 926C-12H-3, 145–146cm). This study recognizes six species of described Amauroliths, *A. primus, A. ninae, A. delicatus, A. amplificus, A. tricorniculatus,* and *A. bizarrus*, and describes one new species, *A. brevigracilis*.

4.3 *Ceratolithus* (See Figure 6)

This group is characterized as a horseshoe-shaped group that is birefringent in XPL. Like the Amauroliths, the Ceratoliths share similar morphological variability. Further subdivision in the *C. acutus* lineage was made based on the arch to horn ratio. The genus appeared just before the end of the Miocene and two species are extant. The primary stratigraphic utility of the genus in both GoM wells and global research is in the lowermost Pliocene. It's been proposed that *Ceratolithus* evolved from *Triquetrorhabdulus* (Raffi *et al*., 1998) in the uppermost Miocene (*C. atlanticus,* 5.389Ma). Major radiation of this lineage occurred across the Miocene/Pliocene boundary in which a minimum of eight taxa evolve over ~410kyr (Figure 6) in the uppermost Messinian to lowermost Zanclean (5.389–4.978Ma). Six taxa have earliest Pliocene extinctions. The base of *C. acutus* observed at 5.340Ma (926A-16H-5, 84–85cm; +/-0.014Ma) defines the lower zonal boundary for Subzone NN12b (Blair *et al*., this paper). This group includes nine taxa with two new species described within the *C. acutus* lineage, *C. apiculus* and *C. cornulum.*

5. Systematic Paleontology

5.1 *Discoaster quinqueramus* lineage (with *C. mexicanus*)

Genus *Discoaster* Tan, 1927

Discoaster abrachiatus Blair & Bergen, *sp. nov.*

Pl. 6, figs 19–31

Derivation of name: L. *brachiatus*: with arms or branches

Diagnosis: Highly birefringent (1st order blues to reds) plug composed of an opposing distal stem and proximal knob and lacking any rays.

Description (lateral view): Small to medium-sized nannolith. Specimens composed of a short conical to cylindrical proximal knob fused to an opposing taller and wider distal stem that appears tulip-shaped. Specimens exhibit high birefringence colors, including 1st order reds and blues. These "plugs" lack any rays. Specimen height to width ratios are equal to or slightly less than the width. Height to width ratios for the proximal stem are 2/3 and the distal knob about 1/2. Size range: height (H) = 4.8–5.6μm; width (W) = 5.0–6.0μm (five specimens).

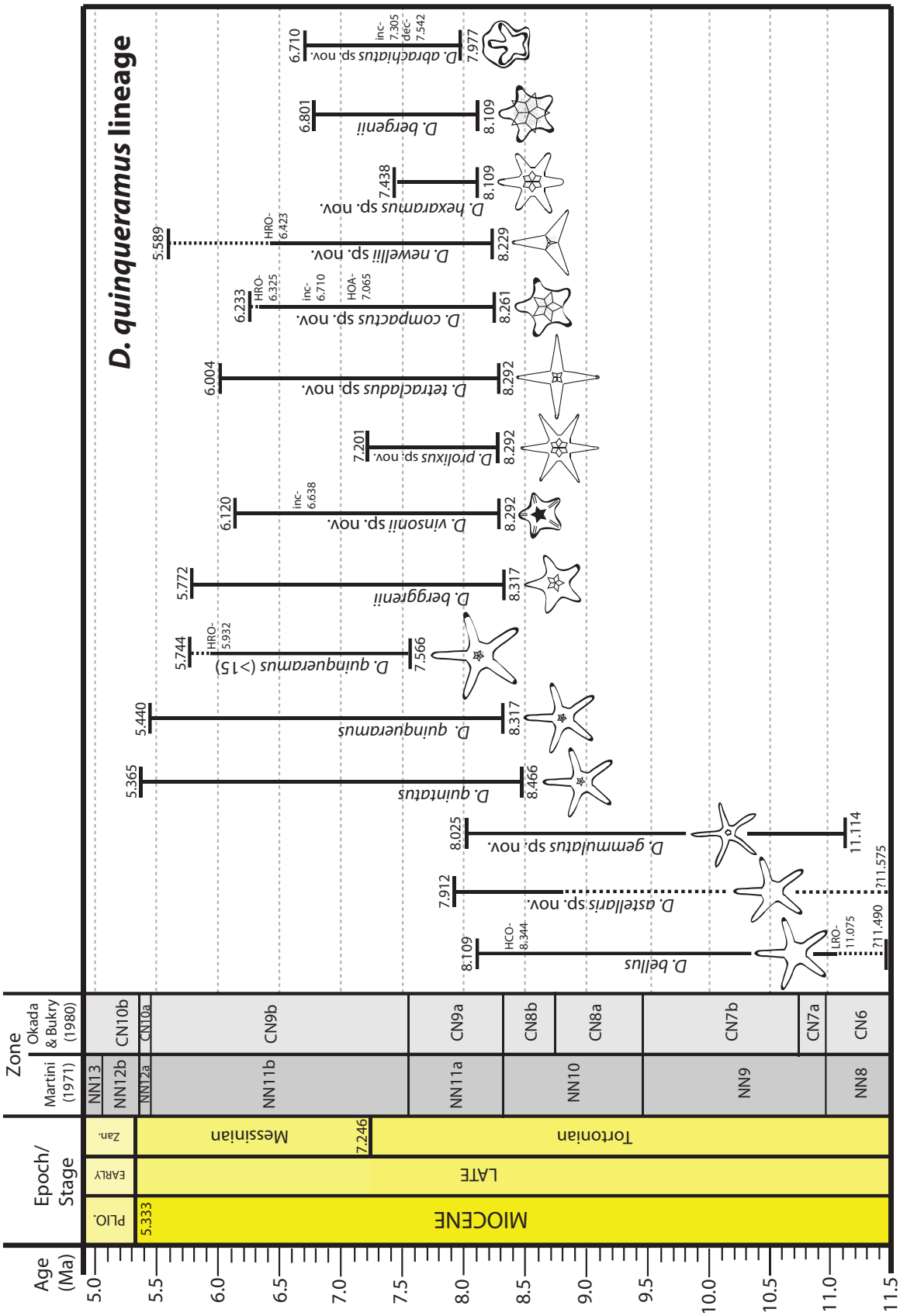

Figure 5: Range diagram of the *Discoaster quinqueramus* lineage. Ranges as well as new ages for the NN (Martini, 1971) and CN (Okada & Bukry, 1980) zonations are derived from calibrated ages in ODP Leg 154 core samples as well as the Gulf of Mexico. Not included in this diagram are *D. consutus* and *D. explicatus* as their extinctions are not yet well-constrained

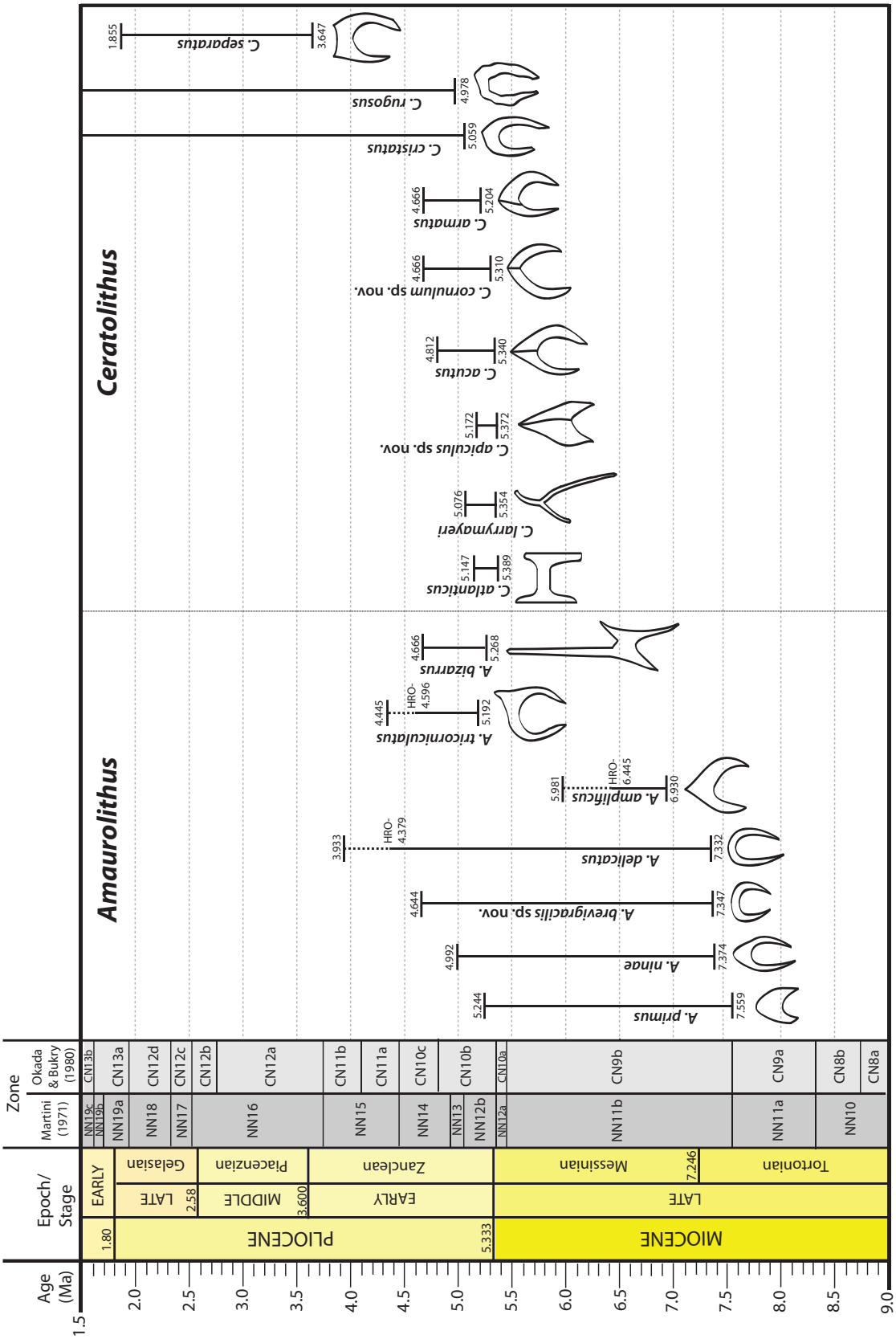

Figure 6: Range diagram of the genera *Amaurolithus* and *Ceratolithus*, including the *C. acutus* lineage. Ranges as well as new ages for the NN (Martini, 1971) and CN (Okada & Bukry, 1980) zonations are derived from calibrated ages in ODP Leg 154 core samples as well as the Gulf of Mexico. Not included in diagram: *C. telesmus*. This figure retains the Pliocene/Pleistocene boundary at the top of the Gelasian because the BP GNATTS framework has not yet adopted the new Pliocene/Pleistocene boundary placement at the base of the Gelasian Stage

Remarks: *Discoaster abrachiatus* was informally known as "*Discoaster pre-berggrenii extreme*" within BP GoM. It is believed equivalent to *Discoaster bergenii* var. A (Da29VarA) on the GCTEP diagram. The high birefringence and lack of rays are diagnostic of this species, which is identified in lateral view. *Discoaster abrachiatus* is believed to be related to the *D. quinqueramus* lineage, even though it lacks any rays. *Discoaster bergenii*, often observed in lateral view, has short arms and its high stems are less birefringent (1st order yellow to orange). Transitional forms between the two species (Pl. 6, figs 14–18) have very short, stubby rays that extend from the "plug", but have the higher blue to red birefringence.

Holotype: Pl. 6, figs 22–23

Type Locality: DSDP Leg 68, Colombia Basin (western Caribbean Sea)

Type Level: Sample 502-48H-1, 90–91cm; Upper Miocene (NN11a)

Occurrence: The HO of *D. abrachiatus* is a long-standing BP GoM marker. This event was dated in Leg 154 materials at 6.710Ma (Table 1). The top and base "acmes" of *D. abrachiatus* are both GoM markers, which have been dated at 7.305Ma and 7.542Ma in the Leg 154 research, respectively (Table 1). In GoM and Leg 154 materials, the LO of *D. abrachiatus* is in mid-Zone NN11a, dated at 7.977Ma (926B-20H-6, 133–134cm; +/-0.026).

Discoaster astellaris Blair & Bergen, *sp. nov.*
Pl. 1, figs 4–7

Derivation of name: L. *stellaris*: of the stars

Diagnosis: A medium-large, simple asterolith with five rays in which the angle between adjacent rays is not equal and lacks any central knob or structure.

Description: This asterolith is characterized by long, straight, asymmetric rays that taper slightly and have pointed-rounded terminations. The free ray length to central area ratio of *Discoaster astellaris* is roughly >1. Specimens measured in this study range between 5.6–10.4μm (holotype is 10.2μm).

Remarks: *Discoaster astellaris* represents an asymmetric *D. bellus*, morphologically separate only in symmetry; however, its distinction is important as this asymmetric form ranges stratigraphically higher than that observed in *D. bellus* (see Occurrence below). *Discoaster gemmulatus* and *D. symmetricus* are distinct from *D. astellaris* in that they both possess central knobs. In *Discoaster hamatus*, the ray terminations are bent and have a prominent spur.

Holotype: Pl. 1, fig. 6

Type Locality: ODP Leg 154, Ceará Rise (western equatorial Atlantic)

Type Level: Sample 926C-22H-1, 128–129cm; Upper Miocene (NN11a)

Occurrence: The HO of *D. astellaris* occurs in Subzone NN11a, dated at 7.912Ma (Table 1), and is a useful event observed in both GoM and Leg 154 materials. *Discoaster astellaris* was consistently observed in Leg 154 samples down to mid-Zone NN10. Below this, its occurrence was spotty to its base, observed at the top of Zone NN7 (11.575Ma; 926A-26H-2, 108–110cm).

Discoaster bellus Bukry & Percival, 1971
Pl. 1, figs 1–3

1971 *Discoaster bellus* Bukry & Percival, p. 128, pl. 3, figs. 1–2

Remarks: *Discoaster bellus* is distinguished from *D. astellaris* by its ray symmetry and from *D. gemmulatus* by its lack of any central area knob or structure. Bukry & Percival (1971) separate *D. bellus* from *D. hamatus* by its "consistently smaller size and lack of large ray-tip spur". Browning *et al.* (this volume) illustrate and define a small form of *Discoaster hamatus*; however, this is separated from *D. bellus* by its well-defined, bent ray-tip spurs. Bukry & Percival (1971) give a size range for *D. bellus* of 8–14μm. Specimens illustrated in this paper measure between 7.2–12.5μm.

Occurrence: *Discoaster bellus* represents a long-standing GoM marker with its extinction in lowermost Subzone N11a. The HO of *Discoaster bellus* in the Gulf of Mexico corresponds to its highest common occurrence in ODP Leg 154, dated at 8.344Ma (Table 1). The known range of *Discoaster bellus* is from NN8-NN11a (Figure 5).

Discoaster bergenii (Knüttel, Russell & Firth, 1989) Blair & Bergen, emend.
Pl. 5, figs 10–17, 21

1984 *Discoaster* sp. cf. *D. berggrenii*. Bergen, p. 431, pl.1, fig. 6

1989 *Discoaster bergenii* Knüttel, Russell & Firth, p. 260, pl.1, fig. 15

2003 *Discoaster bergenii* Knüttel, Russell & Firth. Wei, p. 19, pl.1, fig. 1

Emended description: Medium to large asterolith with five short rays which taper to form pointed to rounded terminations. Free ray length is largely less than 2/3 the diameter of the central area (measured ratios 0.53–0.63). The large central area has both a proximal and distal pentagonal projection (*i.e.,* knob and stem, respectively). The central area diameter is about 1/2 the specimen size (measured ratios 0.45–0.48). The distal stem is stellate, composed of five narrow elements which extend between the rays; these elements extend outside the periphery of the central area. The points of the pentagonal proximal knob are typically aligned with the rays; this knob nearly fills or fills the central area (ratios 0.8–1.0). Size range: 5.0–9.0μm.

Remarks: Bergen (1984) informally described *Discoaster* sp. cf. *D. berggrenii* for "a small, five-rayed asterolith with arms less than half the length of the central area and a distinct stellate knob that entirely fills or extends beyond the central area". The formal description by Knüttel *et al*. (1989) added arm symmetry and a size range of 5–9μm. Wei (2003) mentioned tapered and non-bifurcate

rays, a prominent inter-ray star which frequently extends beyond the central area, and that the free rays are up to half the central area diameter. The proximal knob was omitted in all three of these descriptions. The original species concept of *D. bergenii* was an old Amoco GoM marker known as "*Discoaster* 11 large", which was later separated into two taxa by Amoco that represent *D. bergenii* and *D. compactus*, presented herein. *Discoaster bergenii* is emended to include only forms whose stellate distal stems extend outside the central area periphery. The stem of *D. compactus* fills, but does not extend outside the periphery of the central area. *Discoaster vinsonii* has free ray and central area dimensions comparable to *D. bergenii*, but that species has thick arms with medial distal ridges.

Occurrence: The HO of *D. bergenii* was long utilized as a GoM marker by Amoco. This event was integrated into the post-merger framework in several deep-water BP GoM wells, where its marks a stratigraphic horizon along with the HOs of *Discoaster calcaris* and *D. loeblichii*. This same complex of events was observed in the Leg 154 research, the HO of *D. bergenii* dated at 6.801Ma (Table 1). The LO of *D. bergenii* in Subzone NN11a is dated at 8.109Ma (926B-21H-5, 11–12cm) in Leg 154, roughly equivalent to its position in the GoM.

Discoaster berggrenii (Bukry, 1971) Blair & Bergen, emend.

Pl. 4, figs 1–2

1969 *Discoaster quinqueramus* Gartner (*pro parte*), p. 598, pl. 1, figs. 7; *non* pl. 1, fig. 6

1969 *Discoaster quintatus* Bukry & Bramlette (*pro parte*), p. 133, pl. 1, figs. 6; *non* pl. 1, figs. 7–8

1971 *Discoaster berggrenii* Bukry, p. 45, pl. 2, figs. 4–6

2003 *Discoaster berggrenii* (Bukry, 1971) *berggrenii* Wei, p. 20, pl. 1, figs. 4–5

Emended description: Medium to very large asterolith with five rays that taper to form pointed to rounded terminations. Free ray length is approximately equal to central area diameter with measured ratios between 2/3 to less than 1.2. The central area has both a proximal and distal pentagonal projection. The ratio of central area diameter to specimen size is approximately 1/3 (measured ratios 0.30–0.40). The distal stem is stellate, composed of five narrow elements which extend between the rays and do not fill the central area. The points of the pentagonal proximal knob are typically aligned with the rays. Size range: 8.0–13.0μm.

Remarks: Bukry (1971, p. 45) described *D. berggrenii* as "a symmetric five-rayed asterolith with the free length approximately equal to the diameter of the central area". He also mentioned a proximal star-shaped projection that "practically fills the central area". Bukry (1971) also included a specimen of both *D. quinqueramus* and *D. quintatus* in his synonymy of *D. berggrenii*. Wei (2003) described *D. berggrenii extensus* (see *D. consutus,* this paper) for forms with stems extending beyond the central area periphery and ray lengths 1/2 to equal the central area diameter. He then provided a very short description restricting *D. berggrenii berggrenii* to forms with free ray lengths longer than the central area diameter, leaving no place to classify specimens with shorter arms and smaller stems. *Discoaster berggrenii* is emended herein to rectify any confusion and also to include its proximal knob (see also discussion of *D. consutus*, this paper). *Discoaster berggrenii* is intermediate between *D. quinqueramus* and *D. bergenii* in terms of the ratio of free ray length to central area diameter. *Discoaster berggrenii* is distinguished from *D. quinqueramus* by ratios less than 1.2. *Discoaster bergenii* is reserved for specimens with ratios less than 2/3, but also stellate distal stems that extend outside the central periphery. Specimens with short arms and smaller distal stems have been identified as *D. berggrenii* (Pl. 4, figs 3–5), but may represent a new taxon.

Occurrence: *Discoaster berggrenii* is a classic marker taxon in the GoM used by all three heritage companies, its range restricted to Zone NN11. Both the LO and HO are coeval events in Leg 154 and GoM, dated at 8.317Ma and 5.772Ma (Table 1), respectively.

Discoaster compactus Blair & Bergen, *sp. nov.*

Pl. 4, figs 19–28; Pl. 5, figs 1–3

Derivation of name: L. *compactus*: thick, firm.

Diagnosis: A five-rayed asterolith of the *Discoaster quinqueramus* lineage with short arms and a large center containing a stellate stem whose five elements extend to the periphery of the central area between the rays.

Description: Medium to large asterolith with five short rays which taper to form pointed to rounded terminations. Free ray length is roughly less than 2/3 the diameter of the central area (measured ratios 0.32–0.55). The large central area has both a proximal and distal pentagonal projection. The central area diameter is about 1/2 the specimen size (measured ratios 0.48–0.61). The distal stem is stellate, composed of five narrow elements which extend between the rays; these elements extend to the periphery of the central area. The points of the pentagonal proximal knob are generally aligned with the rays; this knob nearly fills the central area (ratios 0.6–0.9). Measured size range: 5.0–9.2μm.

Remarks: *Discoaster compactus* is reserved for specimens whose stellate stems extend to the periphery of the central area. Specimens with smaller stems and longer arms are referred to as *D. berggrenii*. *Discoaster vinsonii* sp. nov. is another short-armed species within this plexus of forms, but has thick arms with distinct radial distal ridges. Side views of this form can frequently occur in samples (Pl. 5, figs 4–9). Some can even exhibit high birefringence colors similar to *D. abrachiatus* sp. nov.; however, the distinct presence of "rays" distinguishes *D. compactus* from *D. abrachiatus* sp. nov. in side view.

Holotype: Pl. 4, figs 26–28

Type Locality: DSDP Leg 68, Colombia Basin (western Caribbean Sea)

Type Level: Sample 502-48H-1, 90–91cm; Upper Miocene (NN11a)

Occurrence: *Discoaster compactus* was informally known as "*D. berggrenii compactus"* within GoM BP, its HO utilized as a GoM marker within Amoco before the mergers of the three heritage companies. Five events related to the occurrence of this species have been reproduced in sequence in the deep-water GoM, all of which are dated in the Leg 154 research. The stratigraphic range of *D. compactus* is entirely in Zone NN11, its HO dated at 6.233Ma (Table 1). The HRO of *D. compactus* was observed in close proximity to the HO of *Reticulofenestra rotaria* (>5) in the deep-water GoM, the former event dated at 6.325Ma (Table 1). Its first downhole increase has been associated with the HO of *D. abrachiatus* in the GoM and Leg 154, both dated at 6.710Ma (Table 1). The top acme of this subspecies in the GoM is dated at 7.065Ma (Table 1) tied to its highest frequent occurrence in the Leg 154 research. The LO of *D. compactus* is at the base of Subzone NN11a in the Leg 154 research, dated at 8.261Ma (+/-0.031; 926B-21H-5, 127–128cm). Its inception is slightly younger, ~55ky, than that of *D. quinqueramus* (base NN11).

Discoaster consutus Blair & Bergen, *sp. nov.*

Pl. 4, figs 6–18

2003 *Discoaster berggrenii* (Bukry, 1971) *extensus* Wei, p. 20, pl. 1, figs. 2–3

Derivation of name: L. *consuo*: stuff, fill up.

Diagnosis: A five-rayed asterolith of the *Discoaster quinqueramus* lineage with medium length rays and a large center containing a stellate stem whose five elements extend beyond the periphery of the central area between the rays.

Description: Medium to large asterolith with five medium rays which taper to form pointed to rounded terminations. Free ray length to central area ratios are greater than 2/3 to less than one and 1/5 the diameter of the central area. The central area has both a proximal and distal pentagonal projection. The distal stem is stellate, composed of five narrow elements which extend between the rays; these elements extend beyond the periphery of the central area. The points of the pentagonal proximal knob are generally aligned with the rays.

Remarks: We do not employ any taxa below the rank of species within the *D. quinqueramus* lineage. Unfortunately, elevating *D. berggrenii extensus* to species level within *Discoaster* creates a homonym (Article 53.1 in the ICBN) with *Discoaster extensus* Hay (1967). A new name has been given here, *D. consutus*, but the original holotype of Wei (2003) is retained (p. 20, pl. 1, fig. 2). Wei (2003, p. 20) restricted *D. berggrenii extensus* to specimens with "a prominent inter-ray star extending beyond the central area" and free ray lengths between 1/2 to equal to the central area diameter. These ratios are emended herein, partly because the holotype of *D. bergenii* has a free ray length to central area ratio greater than 1/2 (~ 0.6). *Discoaster consutus* is distinguished from *D. bergenii* by its higher free ray length to central area ratio and from *D. explicatus* by its lower free ray length to central area ratio. *Discoaster berggrenii* and *D. compactus* sp. nov. have similar free ray length to central area ratios as *D. consutus*, but their stellate distal stems that do not extend outside the central area periphery.

Occurrence: Historically, this species has not been used in BP GoM taxonomies, its morphotype was lumped in with *D. berggrenii*. In the Leg 154 material, we have identified the LO of *D. consutus*, observed in sample 926B-21H-5, 127–128cm (8.261Ma +/-0.031). We have yet to constrain its top; however, it is restricted to Zone NN11. *Discoaster consutus* was observed in both the GoM and Leg 154 sections.

Discoaster explicatus Blair & Bergen, *sp. nov.*

Pl. 2, figs 4–15

Derivation of name: L. *explicatus*: unrolled, unfolded, spread out.

Diagnosis: A species in the *Discoaster quinqueramus* lineage with five long rays and a stellate distal stem that extends outside central area periphery.

Description: Large to very large asterolith with five long rays. The rays taper to form pointed to rounded terminations. Free ray length is significantly greater than the diameter of the central area (ratio ≥1.2). The small central area has both a proximal and distal pentagonal projection. The ratio of central area diameter to specimen size is less 1/3. The distal stem is stellate, composed of five narrow elements which extend between the rays; these elements extend outside the central area. The points of the pentagonal proximal knob are generally aligned with the rays; this knob nearly fills or extends outside the central area (ratio 0.8–1.4). Measured size range: 10.0–13.0μm.

Remarks: The free ray length to central area ratio of the holotype is about 1.4. Measured specimens range in size from 10.5–12.8μm. This species differs from *D. quinqueramus* by having a distal stellate stem that extends outside of the central periphery. *Discoaster explicatus* is distinguishable from *D. bergenii* and *D. consutus* sp. nov. by having free ray length to central area ratios generally greater than 1.2. Transitional specimens to or from *D. explicatus*-*D. consutus* exist as the rays shorten or lengthen (Pl. 2, figs 16–18).

Holotype: Pl. 2, figs 10–12

Type Locality: DSDP Leg 68, Colombia Basin (western Caribbean Sea)

Type Level: Sample 502-48H-1, 90–91cm; Upper Miocene (NN11a)

Occurrence: Historically, this species has not been used in BP GoM taxonomies, its morphotype was lumped in with *D. quinqueramus*. In the Leg 154 material, we

have identified the LO of *D. explicatus*, observed in sample 926B-21H-6, 32–33cm (8.292Ma +/-0.001). We have yet to constrain its top; however, it is restricted to Zone NN11. *Discoaster explicatus* was observed in both the GoM and Leg 154 sections.

Discoaster gemmulatus Blair & Bergen, *sp. nov.*
Pl. 1, figs 8–10

Derivation of name: L. *gemmula*: bud, dim

Diagnosis: A medium-large, simple, five-rayed asterolith with symmetric, straight rays that slightly taper to pointed-rounded terminations and a small central knob.

Description: *Discoaster gemmulatus* is characterized by long, straight, symmetric rays with a free ray length to central area ratio roughly >1. Also diagnostic to this species is the presence of a proximal circular to subpentagonal central knob that makes up approximately ½ the width of the central area. Specimens measured range in size from 6.8–8.8μm (holotype is 8.0μm).

Remarks: *Discoaster gemmulatus* differs from *D. bellus* by the presence of a central knob. *Discoaster quintatus,* though similar, has a distal stellate stem as opposed to the circular-subpentagonal knob of *D. gemmulatus*. Although asymmetric forms of *Discoaster gemmulatus* were observed (Pl. 1, fig. 11), it is distinct from *D. asymmetricus* and *D. astellaris* by its straight rays and presence of a central knob structure, respectively. Transitional specimens of *D. bellus* to *D. gemmulatus* were observed where it was difficult to determine if a central knob had developed.

Holotype: Pl. 1, figs 9–10

Type Locality: ODP Leg 154, Ceará Rise (western equatorial Atlantic)

Type Level: Sample 926C-22H-3, 77–78cm; Upper Miocene (NN10)

Occurrence: The top of *Discoaster gemmulatus* is a useful event aligned between the extinctions of *D. bellus* and *D. astellaris*. Its HO occurs in Subzone NN11a, dated at 8.025Ma (Table 1). *Discoaster gemmulatus* evolved from its parent taxon, *D. bellus,* in the earliest Tortonian; its LO dated at 11.114Ma (+/-0.019; 926A-25H-6, 70–72cm) in the Leg 154 research.

Discoaster hexaramus Blair & Bergen, *sp. nov.*
Pl. 3, figs 21–30

Derivation of name: L. *hexa*: six and from L. *ramus*: branch.

Diagnosis: *Discoaster* having six straight short rays with simple terminations and two hexagonal projections.

Description: Large to very large asterolith with six short to medium length rays. The rays taper to form pointed to rounded terminations and bend proximally near their terminations. Free ray length is significantly less than the diameter of the central area (measured ratios about 1/2 to three-quarters). The large central area has both a proximal and distal hexagonal projection. The ratio of central area diameter to specimen length is less than to roughly equal to 1/2 (measured 0.40–0.52). The distal stem is stellate, composed of six narrow, tapered elements which extend between the rays; these elements nearly fill or extend outside of the central area. The points of the hexagonal proximal knob are generally aligned with the rays; this knob does not fill the central area. Measured size range: 9.0–14.0μm.

Remarks: *Discoaster hexaramus* represents a six-rayed form within the *D. quinqueramus* lineage. It is distinguished from *D. prolixus* sp. nov. by its relatively shorter rays and larger central area. It is distinguished from other six-rayed *Discoaster* by its radial rays with simple terminations and two hexagonal central area projections.

Holotype: Pl. 3, figs 26–27

Type Locality: Mississippi Canyon Protraction area, Gulf of Mexico

Type Level: Upper Miocene (NN11a)

Occurrence: The biostratigraphic range of *D. hexaramus* was short relative to other taxa in the *D. quinqueramus* lineage. The HO of *D. hexaramus* was utilized as a GoM marker within BP prior to the merger of the three heritage companies. Its HO is coeval in both GoM and Leg 154 sediments and dated at 7.438Ma (Table 1). The LO of the species in Leg 154, in basal Zone NN11, is dated at 8.109Ma (+/-0.024; 926A-21H-5, 52–53cm).

Discoaster newellii Blair & Bergen, *sp. nov.*
Pl. 2, figs 19–28; Pl. 3, figs 1–2

Derivation of name: named in honor of nannofossil biostratigrapher Jim Newell, former BP, USA

Diagnosis: *Discoaster* having three straight, long rays with simple terminations and two trigonal projections.

Description: Medium to large asterolith with three long rays. The narrow rays taper slightly to form pointed to rounded terminations and bend proximally near their terminations. The small central area has both a proximal and distal trigonal projection. The distal stem is stellate, composed of three narrow elements which extend between the rays. The points of the trigonal proximal knob are generally aligned with the rays. Measured size range: 7.6–10.0μm.

Remarks: *Discoaster newellii* is a three-rayed form within the *D. quinqueramus* lineage. It is distinguished from other three-rayed *Discoaster* with long rays by its two central projections and radial rays with simple terminations.

Holotype: Pl. 2, figs 25–28

Type Locality: DSDP Leg 68, Colombia Basin (western Caribbean Sea)

Type Level: Sample 502-48H-1, 90–91cm; Upper Miocene (NN11a)

Occurrence: The range of *D. newellii* is restricted within Zone NN11. In Leg 154 material, the HO is dated at 5.589Ma (+/-0.021; 926C-16H-4, 85–86cm). The HRO of *D. newellii* is a useful marker in both GoM, this horizon dated at 6.423Ma (Table 1). The base of *D. newellii* is also

a useful event dated at 8.229Ma (Table 1) and is coeval in both Leg 154 and GoM sediments.

Discoaster prolixus Blair & Bergen, *sp. nov.*
Pl. 3, figs 11–20

Derivation of name: L. *prolixus*: stretched out long.

Diagnosis: *Discoaster* having six straight long rays with simple terminations and two hexagonal projections.

Description: Large to very large asterolith with six long rays. The rays taper to form pointed to rounded terminations and bend proximally near their terminations. Free ray length is nearly equal to or longer than the diameter of the central area (measured ratios 0.86–1.06). The central area has both a proximal and distal hexagonal projection. The ratio of central area diameter to specimen length is about 1/3 (measured 0.32–0.37). The distal stem is stellate, composed of six narrow, tapered elements which extend between the rays; these elements nearly fill or extend outside of the central area. The points of the hexagonal proximal knob are generally aligned with the rays; this knob does not fill the central area. Measured size range: 10.0–13.0μm.

Remarks: *Discoaster prolixus* is a long, six-rayed form within the *D. quinqueramus* lineage. It is distinguished from *D. hexaramus* by its relatively longer rays and smaller central area. It is distinguished from other six-rayed *Discoaster* by its radial rays with simple terminations and two hexagonal central area projections.

Holotype: Plate 3, figures 13–15

Type Locality: DSDP Leg 68, Colombia Basin (western Caribbean Sea)

Type Level: Sample 502-48H-1, 90–91cm; Upper Miocene (NN11a)

Occurrence: *Discoaster prolixus* has a relatively short stratigraphic range spanning that of ~1 my. Though it is not a traditional marker taxon in the BP GoM framework, the latest research from Leg 154 suggests it may be useful. In Leg 154 materials *D. prolixus* is restricted to NN11a-lowermost NN11b, its HO observed in sample 926B-19H-5, 70–71cm (7.201Ma +/-0.018) and LO in sample 926B-21H-6, 32–33cm (8.292Ma +/-0.001).

Discoaster quinqueramus Gartner, 1969
Pl. 1, figs 21–25; Pl. 2, figs 1–3

1969 *Discoaster quinqueramus* Gartner (*pro parte*), p. 598, pl. 1, figs. 6; *non* pl. 1, fig. 7

1971 *Discoaster quinqueramus* Gartner. Bukry, pl. 1, figs. 6

Remarks: Gartner (1969) described *D. quinqueramus* for symmetrical, five-rayed asteroliths having tapered, proximally bent rays and a five-sided central knob. Theodoridis (1984) accounted for both a pointed and stellate stem for the species. His emendation also included short-armed variants (*D. berggrenii*), as well as those with three, four, and six rays; however, there is stratigraphic merit to subdivide the *D. quinqueramus* group on ray number and free ray length to central area ratios. The ratio of free ray length to central area diameter of the holotype is about 1.9; the species is restricted herein to ratios roughly ≥ 1.2, resulting in central area diameter to specimen size ratios less than 0.3. *Discoaster quinqueramus* is reserved herein for five-rayed specimens with smaller stellate distal stems that do not extend outside the central area periphery. The distal stem of *D. explicatus,* sp. nov. extends outside the central area periphery. *Discoaster quintatus* has a single stem and a younger extinction than *D. quinqueramus*.

Occurrence: The total range of *D. quinqueramus* defines the limits of Zone NN11. The HO of this species has long been utilized as a marker in the GoM by all three heritage companies. The LO of the species has also proved useful and been constrained in several deep-water wells. Both events are coeval in Leg 154, where its range is dated from 8.317 to 5.440Ma (Table 1). BP GoM differentiated large *D. quinqueramus* (>15) as "*D. berggrenii* var.", utilizing its shorter stratigraphic range (Figure 5). The HRO of this large variant is a useful marker horizon dated at 5.932Ma (Table 1). The total range of *D. quinqueramus* (>15) is coeval between GoM and Leg 154, dated from 7.566Ma (+/-0.015; 926B-20H-2, 22–23cm) to 5.744Ma (+/-0.026; 926C-16H-6, 121–122cm).

Discoaster quintatus (Bukry & Bramlette, 1969) Blair & Bergen, emend.
Pl. 1, figs 12–20

1969 Bukry & Bramlette (*pro parte*), pp. 133, pl. 1, fig. 7–8, *non* pl. 1, fig. 6

Emended Description: This five-rayed asterolith has long, straight, symmetric rays that taper near their terminations (Bukry & Bramlette, 1969). Bukry & Bramlette (1969, p. 133) state "There is a star-shaped knob on the concave side, the rays of which bisect the angle between the extended rays of the discoaster". Diagnostic to this medium-large asterolith, is its absence of a central proximal plug. *Discoaster quintatus* has a free ray length to central area ratio roughly >1 and the distal stellate stem can measure greater than 1/2 of the central area. Bukry & Bramlette (1969) give a size range of 8–16μm; however, the holotype measures ~19.5μm. Specimens measured in this study can range smaller (6.5μm).

Remarks: *Discoaster quintatus* was described by Bukry & Bramlette (1969). During its publication, *Discoaster quinqueramus* was published and described by Gartner (1969). Bukry & Bramlette (1969) acknowledged *D. quintatus* as a junior synonym of *D. quinqueramus* (Bukry & Bramlette, 1969, p. 142); however, *D. quintatus* has been long-used by BP and its heritage companies in the GoM as a form distinct and separate from *D. quinqueramus*. It is difficult to tell from the holotype of *D. quintatus* whether it has both a distal stem and proximal knob. While the description of *D. quinqueramus* is also problematic, we restrict forms of *D. quinqueramus* to those that have both a distal stellate stem and a proximal

knob (see *D. quinqueramus* discussion). *Discoaster quintatus* differs in that it only bears the distal stellate stem (Figure 3). *Discoaster quintatus* was informally known as "*Discoaster* sp. 1" within BP GoM.

Discoaster quintatus differs from *D. gemmulatus* sp. nov. by its star-shaped stem. This stellate central structure also separates it from *D. hamatus* and *D. bellus.* Its ray symmetry distinguishes it from *D. astellaris* sp. nov.

Occurrence: The top of *Discoaster quintatus* is important as it marks the extinction of the *D. quinqueramus* lineage. It is also a key event for picking the top of the Miocene, its HO observed at 5.365Ma (Table 1), approximately 30kyr below the Miocene/Pliocene boundary. Separating *D. quintatus* (HO-5.365Ma) from *D. quinqueramus* (HO-5.440Ma) has a significant impact when picking top Miocene in the Gulf of Mexico where sedimentation rates can be notably high. The total range of *D. quintatus* is NN12a-NN10 (8.466Ma; 926C-22H-3, 77–78cm), its LO occurs approximately 150kyr below the base of *D. quinqueramus*.

Discoaster tetracladus Blair & Bergen, *sp. nov.*
Pl. 3, figs 3–10

Derivation of name: Gr. *tetra*: four and *klados*: branch.

Diagnosis: *Discoaster* having four straight, long rays with simple terminations and two quadrate projections.

Description: Large asterolith with four long rays. The narrow rays taper slightly to form pointed to rounded terminations and bend proximally near their terminations. Free ray length is nearly equal to or much longer than the diameter of the central area. The central area has both a proximal and distal quadrate projection. The distal stem is stellate, composed of four narrow elements which extend between the rays. The points of the quadrate proximal knob are generally aligned with the rays. Measured size range: 8.4–10.8μm.

Remarks: *Discoaster tetracladus* is a four-rayed form within the *D. quinqueramus* lineage. It is distinguished from other four-rayed *Discoaster* with long rays by its two quadrate projections and radial rays with simple terminations.

Holotype: Pl. 3, figs 3–5

Type Locality: DSDP Leg 68, Colombia Basin (western Caribbean Sea)

Type Level: Sample 502-50H-1, 19–20cm; Upper Miocene (NN11a)

Occurrence: The range of *D. tetracladus* is not well constrained in the GoM, but appears roughly coincident with the stratigraphic range of *D. newellii* sp. nov. *Discoaster tetracladus* is a rare taxon, but was observed in 19 different Leg 154 samples ranging from 8.292Ma (926B-21H-6, 32–33cm) to 6.004Ma (926B-17H-5, 139–140cm).

Discoaster vinsonii Blair & Bergen, *sp. nov.*
Pl. 5, figs 22–30; Pl. 6, figs 1–13

Derivation of name: in honor of BP petrophysicist and manager Graham "Pinky" Vinson.

Diagnosis: A compact, five-rayed asterolith of the *Discoaster quinqueramus* lineage with short, thick, tapered arms that thin to form medial distal ridges.

Description: Small to large asterolith with five broad, short rays. The rays taper to form pointed to rounded terminations. The rays thin peripherally from the thick center, as well as proximally, forming medial distal ridges along their lengths. Free ray length is less than the diameter of the central area (ratio 0.22–0.50). The large central area has both a proximal and distal pentagonal projection. The ratio of central area diameter to specimen size is about 1/2 to 2/3. The distal stem is stellate, composed of five narrow elements which extend between the rays; these elements nearly fill or fill the central area (periphery 0.7–1.0 of central area). The points of the pentagonal proximal knob are aligned with the rays; this knob nearly fills the central area (ratio 0.75–0.90). Size range: 4.8–9.6μm.

Remarks: *Discoaster vinsonii* was informally known as "*Discoaster pre-berggrenii*" within BP GoM. It is believed equivalent to Discoaster 7 (Da7) on the GCTEP diagram. The short, thick rays of *D. vinsonii*, which thin to form distal ridges, are diagnostic and distinguish the species from all other members of the *D. quinqueramus* lineage. The ratio of the short arms to the large central area falls within that of *D. bergenii*. A transitional specimen to *D. berggrenii* is illustrated on Pl. 5, figs 18–20 with less prominent ridges, relatively longer arms (ratio 0.75 to central diameter), and smaller center (0.40 of specimen size).

Holotype: Pl. 5, figs 27–28

Type Locality: DSDP Leg 68, Colombia Basin (western Caribbean Sea)

Type Level: Sample 502-48H-1, 90–91cm; Upper Miocene (NN11a)

Occurrence: The HO of "*D. pre-berggrenii"* was utilized as a GoM marker within BP long before the mergers of the three heritage companies. This event, now the HO of *D. vinsonii*, is dated at 6.120Ma (Table 1) in Leg 154. Its first downhole abundance increase in deep-water wells is tied to its highest frequent occurrence in Leg 154; this event is dated at 6.638Ma (Table 1). The LO of *D. vinsonii* is at the base of Zone NN11 in Leg 154 and dated at 8.292Ma (Table 1), roughly coeval to its appearance in the GoM.

Genus *Catinaster* Bukry, 1971
Catinaster mexicanus Bukry, 1971
Pl. 7, figs 1–30

1971 *Catinaster mexicanus* Bukry, p. 50, pl. 3, figs. 7–9

Remarks: Bukry (1971) described *C. mexicanus* as having six short bifurcate rays and a large central area with a prominent central structure of six ribs extending radially to the interray areas. We have observed variation in the orientation and morphology of these "ribs", which can be aligned with the six short rays and also appear as bifurcate arms of a *Discoaster*; however, we have not been able to place morphologic

variation in context of the stratigraphy of this short-ranging species. In side view, the angular nature of *C. mexicanus* further distinguishes it from other known members of the genus. *Catinaster mexicanus* was described from the GoM. There is an approximately 1.8-myr gap between the appearance of *C. mexicanus* and the extinction of the *Catinaster coalitus* lineage in both the GoM and the Leg 154 research. We feel the origin of *C. mexicanus* may be related to the explosive radiation in the *D. quinqueramus* lineage, which includes a 6-rayed species (*D. hexaramus*), instead of being related to other *Catinaster* species. The stratigraphic range of *C. mexicanus* fits within the range of *D. hexaramus*. The specimen illustrated on Pl. 7, figs 26–27 is from the base of the range of *C. mexicanus*. Similar evolution strategies from *Discoaster-Catinaster* have been detailed in this volume (de Kaenel *et al*., 2017). Aubry (2015) described the genus *Myrsaster* for only *Catinaster mexicanus*. We have observed several iterations of basket-shaped forms associated with radiations of *Discoaster* with high stems during the Middle-Late Miocene in the GoM. We prefer to retain the genus *Catinaster* for all these basketlike forms. Bukry gave a size range of 5–8μm for the species, but we have observed specimens as large as 10.0μm.

Occurrence: *Catinaster mexicanus* is a short-ranging taxon, its entire range spanning ~660ky. The HO of *C. mexicanus* is a standard marker in the GoM utilized by all three heritage companies; this stratigraphic horizon has been dated at 7.566Ma (Table 1). The LO of *C. mexicanus* is also a useful marker event dated at 8.204Ma (Table 1).

5.2 Amaurolith lineage

Genus *Amaurolithus* Gartner & Bukry (1975)

Amaurolithus amplificus (Bukry & Percival, 1971) Gartner & Bukry, 1975

Pl. 9, figs 1–3, 7–8

1971 *Ceratolithus amplificus* Bukry & Percival, p. 125, pl. 1, figs. 9–11

1973 *Ceratolithus dentatus* Bukry, p. 676, pl. 2, figs. 1–3

1975 *Amaurolithus amplificus* (Bukry & Percival, 1971) Gartner & Bukry, p. 454, fig. 6g-l

Remarks: Bukry & Percival (1971, p. 125) mentioned that "one arm, generally that bearing a row of simple tooth-like structures, is straighter than the other, which has a slight inward bend toward the tip". Gartner & Bukry (1974) emended the species to emphasize the short, thick apical spine located above the larger of the two horns and a shorter horn that is sharply curved at its tip. We consider the sub-angular shape of *A. amplificus* diagnostic, especially the broad and noded longer horn. *Amaurolithus tricorniculatus* has slender curved horns and a prominent apical spine. Bukry & Percival (1971) gave a size range of 12–20μm for the species, but Gartner & Bukry (1975) later included specimens as small as 10μm. Smaller specimens have been observed in the GoM and Leg 154 research material as well (See Pl. 9, figs 7–8).

We've retained *A. amplificus* in the *Amaurolithus* genus as opposed to the monospecific genus, *Nicklithus* Raffi *et al.* (1998). The authors believe there is support that the progenitor of *A. amplificus* was likely *Amaurolithus primus*, as opposed to *Triquetrorhabdulus* as suggested by Raffi *et al.* (1998). Therefore, description of a new genus seems unwarranted.

Occurrence: The HO of *A. amplificus* has been dated at 5.981Ma (+/-0.021; 926B-17H-5, 88–89cm) in the Leg 154 research. In Leg 154, the species is persistent in samples through Subzone NN11b, dated from 6.445Ma (HRO; Table 1) to 7.065Ma (LO; Table 1). The HO of *A. amplificus* is utilized as a GoM marker and has been calibrated to its first downhole increase in the Leg 154 research, dated at 6.445Ma (Table 1).

Amaurolithus bizarrus (Bukry, 1973) Gartner & Bukry, 1975

Pl. 9, figs 4–6

1973 *Ceratolithus bizarrus* Bukry, p. 676, pl. 1, figs. 6–10

1975 *Amaurolithus bizarrus* (Bukry & Percival, 1971) Gartner & Bukry, p. 456, fig. 8a–b

Remarks: Bukry (1973) distinguished this species from all others in this group by its complex structure, "typically having two horseshoe-shaped structures attached together along a rod". He also noted intact specimens can be 40–50μm, but the width is 7–12μm.

Occurrence: We do not find *A. bizarrus* to have stratigraphic utility in the GoM. In Leg 154, it is restricted to the Lower Pliocene (NN12b-NN14) and dated from 5.268Ma (+/- 0.009; 926A-16H-4, 75–76cm) to 4.666Ma (+/- 0.022; 926B-14H-6, 30–31cm).

Amaurolithus brevigracilis Blair & Bergen, *sp. nov.*

Pl. 8, figs 9–12

1971 *Ceratolithus primus* Bukry & Percival (*pro parte*), p. 126, pl. 1, fig. 14, *non* pl. 1, figs. 12–13

1975 *Amaurolithus primus* (Bukry & Percival), Gartner & Bukry (*pro parte*), p. 457, fig. 7h, j; *non* fig. 7g, i–l

Derivation of name: L. *brevis*: short and *gracilis*: slender.

Diagnosis: equidimensional, horseshoe-shaped amaurolith with a narrow arch and horns.

Description: Simple, horseshoe-shaped amaurolith. Specimens are roughly equidimensional. The arch is narrow and rounded. The horns are thin and pointed. A short apical spur may be present. Specimens are not birefringent in cross-polarized light. Specimens measured and two illustrated herein have: (1) height to width ratios of 1.00–1.07; (2) arch breadth to specimen height ratios of 0.25–0.28; and (3) a size range of 5.4–9.0μm.

Remarks: *Amaurolithus brevigracilis* is a short form of *A. delicatus*, which is more elongate. *Amaurolithus primus* has a very broad arch. *Amaurolithus tricorniculatus* has an apical spine.

Holotype: Pl. 8, figs 11–12

Type Locality: ODP Leg 154, Ceará Rise (western equatorial Atlantic)

Type Level: Sample 926B-19-5, 100cm; Upper Miocene (NN11b)

Occurrence: In the historical BP GoM, the stratigraphic range of *A. brevigracilis* had been included within that of the longer ranging *A. delicatus*; however, their disparate ranges make it a biostratigraphically-useful morphologic split. In Leg 154, it ranges from the uppermost Miocene (base NN11b) to Lower Pliocene (NN14), where it is dated from 7.347Ma (+/-0.027; 926A-20H-2, 64–65cm) to 4.644Ma (+/-0.020; 926B-14H-5, 120–121cm).

Amaurolithus delicatus Gartner & Bukry, 1975
Pl. 8, figs 13–19

1975 *Amaurolithus delicatus* Gartner & Bukry (*pro parte*), p. 456–457, fig. 7a–e, *non* fig. 7f

Remarks: *Amaurolithus delicatus* and *A. brevigracilis* sp. nov. are both simple forms with narrow, rounded arches and horns. *Amaurolithus brevigracilis* sp. nov. is equidimensional, whereas *A. delicatus* is elongate. *Amaurolithus ninae* is also elongate, but has a broad and pointed arch.

Occurrence: The LO of *A. delicatus* is near the base of Subzone NN11b and is dated at 7.332Ma (Table 1) in Leg 154. Its extinction - also that of the genus *Amaurolithus* - is coeval in the GoM and Leg 154 (top NN15) and dated at 3.933Ma (Table 1). The HRO of *A. delicatus* is much more reliable event in the GoM and coeval in Leg 154, dated at 4.379Ma (Table 1).

Amaurolithus ninae Perch-Nielsen, 1977
Pl. 8, figs 20, 29–30

1975 *Amaurolithus delicatus* Gartner & Bukry (*pro parte*), p. 456, fig. 7f, *non* fig. 7a–e

1977 *Amaurolithus ninae* Perch-Nielsen, p. 745, pl. 1, fig. 4; pl. 2, figs. 9, 14; pl. 4, figs. 3, 6–15; pl. 5, fig. 9, 12–14, pl. 49, fig. 5

Remarks: Perch-Nielsen (1977) diagnosed *A. ninae* as a "ceratolith with a well-developed apical region and two unequal or subequal long horns". She then described it as being non-birefringent, which distinguishes it from all *Ceratolithus*. *Amaurolithus primus* has a well-developed apical region, but it is not pointed like that of *A. ninae*. We are not sure if all 18 electron photomicrographs of *A. ninae* illustrated by Perch- Nielsen (1977) are actually this species; she illustrated a single light photomicrograph in transmitted light.

Occurrence: To date, we do not find *A. ninae* to have stratigraphic utility in the GoM. In Leg 154, the species ranges from Upper Miocene (lower NN11b) to Lower Pliocene (NN13), dated from 7.374Ma (+/-0.028; 926B-20H-2, 134–135cm) to 4.992Ma (+/-0.014; 926B-15H-5, 40–41cm). Its type locality, DSDP Site 354, is located on the Ceará Rise near the Leg 154 sites.

Amaurolithus primus (Bukry & Percival, 1971) Gartner & Bukry, 1975
Pl. 8, figs 1–8

1971 *Ceratolithus primus* Bukry & Percival (*pro parte*), p. 126, pl. 1, figs. 12–13; *non* pl. 1, fig. 14

1975 *Amaurolithus primus* (Bukry & Percival) Gartner & Bukry (*pro parte*), p. 457, fig. 7g, i–l; *non* fig. 7h, j

Remarks: Bukry & Percival (1971, p. 126) stated that *A. primus* is "characterized by short arms and very thick arch". The arch on all three original specimens illustrated by Bukry & Percival (1971) is flat, as opposed to the pointed arch of *A. ninae*. *Amaurolithus brevigracilis* sp. nov. differs by having a narrow arch. Specimens measured and four illustrated herein have height to width ratios of 0.93–1.44 and arch breadth to total height ratios of 0.42–0.79. In this study, transitional forms between *A. delicatus* and *A. primus* were observed (Pl. 8, figs 21–22).

Occurrence: *Amaurolithus primus* has limited stratigraphic utility in deep-water GoM because it is extremely rare. Bukry & Percival (1971) stated the species was restricted to the lower part of the *Ceratolithus tricorniculatus* Zone (CN10a) within the Upper Miocene (or basal NN12). In Leg 154, it was observed in the uppermost Miocene where it defines the base of Subzone NN11b. *Amaurolithus primus* is restricted to NN11b-lowermost NN12 where its range is dated from 7.559Ma (Table 1) to 5.244Ma (+/-0.012; 926A-16H-4, 15–16cm). Its distinction from the short-horned Amaurolith, *A. brevigracilis* sp. nov., is important as this taxon does range into the Lower Pliocene.

Amaurolithus tricorniculatus (Gartner, 1967) Gartner & Bukry, 1975
Pl. 8, figs 23–28

1967 *Ceratolithus tricorniculatus* Gartner, p. 5, pl. 10, figs. 4–6

1975 *Amaurolithus tricorniculatus* (Gartner, 1967) Garner & Bukry, p. 457, fig. 8c-h

Remarks: There is considerable variation in this species, including shape, height to width ratio, and the location of its diagnostic apical spine. The horns, arch, and apical spine of *A. tricorniculatus* are thin and pointed. *Amaurolithus amplificus* has a broader arch, more angular nature, and apical spur - but can sometimes be difficult to distinguish from *A. tricorniculatus*. *Amaurolithus bizarrus* is distinguished by its long, straight rod.

Occurrence: The HO of *A. tricorniculatus* has been utilized by all three heritage companies in the GoM for decades. This short-ranging taxon is restricted to the Lower Pliocene (NN12b-base NN15). Its HO defines the base of Zone NN15, dated at 4.445Ma (Table 1). The HRO of *A. tricorniculatus* is also utilized in the GoM and is coeval is Leg 154 material, dated at 4.596Ma (Table 1). Its base was constrained in Leg 154 material and dated at 5.192Ma (+/-0.012; 926A-16H-3, 55–56cm).

5.3 Ceratolith lineage

Genus *Ceratolithus* Kamptner, 1950

Ceratolithus acutus Gartner & Bukry, 1974

Pl. 10, figs 18–22

1974 *Ceratolithus acutus* Gartner & Bukry, p. 115, pl. 1, figs. 1–4.

1975 *Ceratolithus acutus* Gartner & Bukry, 1974. Gartner & Bukry, p. 458, fig. 6a–f.

1978 *Ceratolithus acutus* Gartner & Bukry, 1974; Bergen (*pro parte*), p. 430, pl. 3, figs. 1–2; *non* figs. 3–6.

Remarks: Gartner & Bukry (1975, p. 458) stated that the "apical structure can be slightly asymmetrical, but typically is a ridge symmetrically aligned with the bisectrix line between the two horns." This apical symmetry and pointed spine are considered diagnostic for the species. Three species are recognized herein in the *Ceratolithus acutus* lineage, based on the ratio of the height of the apical spine to the total length of the specimen, *C. acutus, C. apiculus* sp. nov. and *C. cornulum* sp. nov. *Ceratolithus acutus* is intermediate between the other two species. Specimens measured and illustrated herein have apical spine to total height ratios between 0.43–0.54.

Occurrence: *Ceratolithus acutus* evolved from *C. apiculus* sp. nov. Its appearance is coeval in the GoM and Leg 154, essentially marking the base of the Pliocene, and is dated at 5.340Ma (Table 1) in Leg 154. The HO is dated at 4.812Ma (Table 1) in Leg 154 and is also coeval in the GoM.

Ceratolithus apiculus Blair & Bergen, *sp. nov.*

Pl. 10, figs 6–17

1984 *Ceratolithus acutus* Gartner & Bukry, 1974; Bergen (*pro parte*), p. 430, pl. 3, figs. 5–6, *non* figs. 1–4

Derivation of name: L. *apiculus* (dim.): apex.

Diagnosis: A species within the *Ceratolithus acutus* lineage with a very high, pointed apical spine and short horns.

Description: Large ceratolith having a very high, pointed apical spine. The ratio of the height of the apical spine to the total height of the specimen is 0.55–0.70. An apical suture divides specimens along the longitudinal median. Two short horns extend from the apical spine, curving slightly and tapering to points; their lengths are equal to highly unequal. Specimens become brightly birefringent when rotated in cross-polarized light. Length: 8.8–11.7μm (eight specimens).

Remarks: *Ceratolithus apiculus* is the oldest of the three species in the *C. acutus* lineage, recognized herein, whose evolution lengthens the horns at the expense of reducing the apical region height. This species is distinguished from all other *Ceratolithus* by its very thick apical spine and short horns. *Ceratolithus acutus* also has a thick apical spine, but it is less than 0.55 the total height of the specimen.

Holotype: Pl. 10, figs 9–11

Type Locality: DSDP Leg 68, Colombia Basin (western Caribbean Sea)

Type Level: Sample 502-34H-1, 53–54cm; Lower Pliocene (NN12a)

Occurrence: *Ceratolithus apiculus* is a short-ranging taxon, its entire range spanning ~200kyr. The HO of this species is a marker in the GoM and coeval in Leg 154, where it was dated at 5.172Ma (Table 1). It ranges just into the terminal Miocene at ODP Leg 154 within Subzone NN12a, where its appearance is dated at 5.372Ma (Table 1).

Ceratolithus armatus Müller, 1974

Pl. 11, figs 4–15

1974 *Ceratolithus armatus* Müller, p. 591, pl. 11, figs. 4–6; pl. 19, figs. 3–4.

1975 *Ceratolithus armatus* Müller, 1974. Gartner & Bukry, 1975, p. 458, fig. 5f–i.

1984 *Ceratolithus armatus* Müller, 1974. Bergen, p. 430, pl. 2, figs. 10–11.

Remarks: The original description of this species by Müller (1974) is inadequate to distinguish it from other Ceratoliths. Gartner & Bukry (1975) gave a much more detailed description of the species and stressed the importance of its pointed and asymmetric apical region. Müller (1974) gave a size range of 15–18μm for *C. armatus*. The twelve specimens cited and illustrated herein range between 8.0–17.5μm in length and the height of their apical regions vary between 0.20–0.40 of the total specimen length. This apical height to length ratio is similar to that of *C. cornulum*, but species with the *C. acutus* lineage have a symmetric pointed arch divided by a medial longitudinal suture. Transitional forms between *C. armatus* and *C. cornulum* sp. nov. have been observed (Pl. 11, figs 1–3).

Occurrence: The HO of *C. armatus* is coeval in the GoM and Leg 154, dated at 4.666Ma (Table 1). The LO is not utilized in the GoM, but dated at 5.204Ma (+/-0.028; 926A-16H-3, 75–76cm) in Leg 154.

Ceratolithus atlanticus Perch-Nielsen, 1977

Pl. 9, figs 9–14; Pl. 10, figs 1–5

1977 *Ceratolithus atlanticus* Perch-Nielsen, p. 745, pl. 3, fig. 1–14; pl. 5, figs. 1–7, 10; pl. 49, fig. 2–4

Remarks: Perch-Nielsen (1977) diagnosed *C. atlanticus* as a "ceratolith with a long, straight rod forming an apical spine and a horn of the ceratolith. The other horn and apical spine are shorter." No other ceratolith has these angular features, asymmetry, and two apical spines.

Occurrence: *Ceratolithus atlanticus* has a very short stratigraphic range (~240ky). It is often absent in deep-water GoM sections because of a prominent Miocene/Pliocene boundary unconformity. Its presence in Leg 154 material was consistent ranging from 5.389Ma to 5.147Ma (Table 1), its entire range restricted to Zone NN12. This is consistent with its range in the GoM.

Ceratolithus cornulum Blair & Bergen, *sp. nov.*
Pl. 10, figs 23–30

1984 *Ceratolithus acutus* Gartner & Bukry, 1974. Bergen (*pro parte*), p. 430, pl. 3, figs. 3–4, *non* figs. 1–2, 5–6

Derivation of name: L. *cornulum* (dim.): horn.

Diagnosis: A species within the *Ceratolithus acutus* lineage with a thin, pointed apical region and long, curved horns.

Description: Large ceratolith having a very low apical region. The ratio of the height of the apical spine to the total height of the specimen is 0.25–0.40. An apical suture divides specimens along the longitudinal median. Two long horns extend from the apical spine, curving inward and tapering to points; their lengths are equal to highly unequal. Specimens become brightly birefringent when rotated in cross-polarized light. Size: 9.6–11.7μm (five specimens).

Remarks: *Ceratolithus cornulum* is distinguished from the other two species of *C. acutus* lineage by its relatively low apical spine. The apical spine of *C. armatus* has the same relative height, but the apical suture of that species is not aligned with the longitudinal median.

Holotype: Pl. 10, figs 25–26

Type Locality: DSDP Leg 68, Colombia Basin (western Caribbean Sea)

Type Level: Sample 502-31H-2, 123–124cm; Lower Pliocene (NN12b)

Occurrence: *Ceratolithus cornulum* is the youngest taxon within the *C. acutus* lineage in both the GoM and Leg 154, the LO being dated in the latter at 5.310Ma (Table 1). In the GoM and Leg 154, the HO is coincident with that of *C. armatus*, dated at 4.666Ma (+/-0.022; 926B-14H-6, 30–31cm).

Ceratolithus cristatus Kamptner, 1954 emended Bukry & Bramlette, 1968
Pl. 11, figs. 16–23, 26–29

1954 *Ceratolithus cristatus* Kamptner, p. 43, textfigs. 44–45.

1968 *Ceratolithus cristatus* Kamptner. Bukry & Bramlette, p. 150, pl. 1, figs. 1–4.

Remarks: *Ceratolithus cristatus* has a flat to slightly rounded arch with two long horns; the species is asymmetric, in that one side of the ceratolith is higher than the other. *Ceratolithus telesmus* has longer horns whose tips are closer together. *Ceratolithus separatus* is bilaterally symmetrical, has a saddle-shaped arch and numerous spines extending from its body.

Occurrence: *Ceratolithus cristatus* is extant, but its appearance is useful in the GoM. The LO of this species marks the base of Zone NN13 herein and also utilized in deep-water GoM wells. The appearance of this species is dated from Leg 154 research, dated at 5.059Ma (Table 1).

Ceratolithus larrymayeri Backman & Raffi
Pl. 9, figs 15–18

1998 *Ceratolithus larrymayeri* Backman & Raffi, *in* Raffi, Backman & Rio, p. 39, pl. 6, figs. 10, 15–16; pl. 7, figs. 3–4

Remarks: Raffi *et al.* (1998) stated that *C. larrymayeri* has a "much more delicate and slender nature" than other *Ceratolithus* from the Miocene/Pliocene boundary interval. Its morphology is more reminiscent of *A. tricorniculatus*, which is not birefringent.

Occurrence: Although a very distinct species with a short stratigraphic range, we have not yet established a calibrated stratigraphic range for *C. larrymayeri* in the GoM. Raffi *et al.* (1998) reported the range of this species straddling the Miocene/Pliocene boundary in five Leg 154 sites, stating an age of 5.37 to 5.26Ma in upper Zone NN12. We have observed the species in 18 samples from 926A-16H-5, 105–106cm (5.354Ma +/-0.008) to 926B-15H-6, 100–101cm (5.076Ma +/-0.017), its inception just ~20ky below the Miocene/Pliocene boundary.

Ceratolithus rugosus Bukry & Bramlette, 1968
Pl. 12, figs 5–8

1968 *Ceratolithus rugosus* Bukry & Bramlette, p. 152, pl. 1, figs. 5–9

Remarks: *Ceratolithus rugosus* is a horseshoe-shaped ceratolith characterized by its rugose surface. No other ceratolith shares this feature, although we are not entirely sure if this rugose nature is not related to preservation (Bergen, 1984). The holotype has a rounded arch and long horns that are parallel. The horns may also curve inward or extend outward, as illustrated herein.

Occurrence: We were not able to establish a reliable stratigraphic range for *C. rugosus* in the GoM because it is extremely rare in wells. In ODP Leg 154, the LO was dated at 4.978Ma (+/-0.014; 926B-15H-5, 2–3cm). The LO of this species traditionally marked the base of Zone NN13 (Martini, 1971) and Subzone CN10c (Okada & Bukry, 1980); however, due to the uncertainty of its preservational morphology, we proposed the LO of *C. cristatus* (5.059Ma) as a better zonal candidate (see Biostratigraphy section, above).

Ceratolithus separatus Bukry, 1979
Pl. 12, figs 9–21

1979 *Ceratolithus separatus* Bukry, p. 310, pl. 1, figs. 1–16.

Remarks: Bukry (1979) mentioned that the arch of *C. separatus* is very broad and has a saddle-like appearance. The two horns are thick, subparallel, and both ornamented by nodes or keels. Bukry (1979) gave a size range of 14–20μm for the species; we have illustrated specimens as small as 10.0μm.

Occurrence: The HO of *C. separatus* was utilized by Amoco as a GoM marker, observed between the HOs of *Discoaster brouweri* and *Calcidiscus macintyrei* in the lowermost Pleistocene. In Leg 154, its HO occurs in lowermost Subzone NN19a, dated at 1.855Ma (+/-0.023; 926C-6H-3, 144–145cm); the LO was observed in lower NN16 and dated at 3.647Ma (+/-0.019; 926C-11H-5, 123–124cm).

Ceratolithus telesmus Norris, 1965
Pl. 12, figs 1–4
1965 *Ceratolithus telesmus* Norris, p. 21, pl. 11, figs. 5–7; pl. 13, figs. 1–3

Remarks: *Ceratolithus telesmus* is characterized by its high height to width ratio, rounded arch, and horns which nearly touch at their tips.

Occurrence: This appearance of this extant species has not been established in GoM wells. In Leg 154, its LO has been dated at 4.838Ma (+/-0.020; 926B-15H-2, 50–51cm).

Acknowledgements

We are grateful to BP GoM Exploration for their support and encouragement in the publication of this research as well as Graham Vinson, Liz Jolley, and John Farrelly. We are appreciative of the BP GoM teams in Exploration and Production. These groups were fundamental in integration and application of these biostratigraphic events for subsurface description. Special thanks are extended to Jim Newell, whose work for two of the BP heritage companies contributed greatly to this work. The authors would like to also thank BP for its financial support of the ODP Leg 154 sampling and research as well those involved with the acquisition, preparation, and analyses of materials involved in this study. We're also grateful to the Integrated Ocean Drilling Program for the use of ODP Leg 154 materials. Our gratitude is extended to Drs. David Watkins and James Pospichal for reviewing this manuscript. Of course we'd like to thank the authors' families for their patience and support as these five papers were concurrently written and reviewed. Finally, it has not been lost on the authors that these five papers introduce a beastly barrage of brand-new bugs, their authors beginning with B. Not since Wind & Wise *in* Wise & Wind (1977) has this had the potential for confusion. From Blair, Bergen, Browning and Boesiger… we apologize, briefly.

References

Aubry, M.-P. 2015. *Cenozoic coccolithophores: Discoasterales* (CC-E). Atlas of Micropaleontology Series. Micropaleontology Press, New York: 532 pp.

Bergen, J.A. 1984. Calcareous nannoplankton from Deep Sea Drilling Project Leg 78A: evidence for imbricate underthrusting at the Lesser Antillian active margin. *In*: B. Biju-Duval, J.C. Moore, *et al., Initial Reports of the DSDP*, **78**: Washington D.C. (U.S. Government Printing Office): 411–445.

Bergen, J.A., de Kaenel, E., Blair, S., Boesiger, T., & Browning, E. 2017. Oligocene-Pliocene taxonomy and stratigraphy of the genus *Sphenolithus* in the circum North Atlantic Basin: Gulf of Mexico and ODP Leg 154. *Journal of Nannoplankton Research,* **37** (2/3), 77–112.

Bergen, J.A., Truax III, S., de Kaenel, E., Blair, S., Browning, E., Lundquist, J., Boesiger, T., Bolivar, M., & Clark, K. 2017 (in prep). BP Gulf of Mexico Neogene Astronomically-tuned Time Scale.

Boesiger, T., de Kaenel, E., Bergen, J., Browning, E., & Blair, S. 2017. Oligocene to Pleistocene taxonomy and stratigraphy of the genus *Helicosphaera* and other placolith taxa in the circum North Atlantic Basin. *Journal of Nannoplankton Research*, **37**(2/3), 145–175.

Browning, E., Bergen, J., Blair, S., de Kaenel, E. & Boesiger, T. 2017. Late Miocene to Late Pliocene taxonomy and stratigraphy of the genus *Discoaster* in the circum North Atlantic Basin: Gulf of Mexico and ODP Leg 154. *Journal of Nannoplankton Research*, **37**(2/3), 189–214.

Bukry, D. 1971. *Discoaster* evolutionary trends. *Micropaleontology*, **17**(1): 43–52.

Bukry, D. 1973. Coccolith stratigraphy, eastern equatorial Pacific, Leg 16 Deep Sea Drilling Project. *In*: T.H. van Andel, G.R. Heath *et al*., *Initial Reports of the DSDP*, **16**: Washington D.C. (U.S. Government Printing Office): 653–711.

Bukry, D. 1979. Neogene coccolith stratigraphy, mid-Atlantic Ridge, Deep Sea Drilling Project Leg 45. *In*: W.G. Melson, P.D. Rabinowitz *et al*., *Initial Reports of the DSDP*, **45**: Washington D.C. (U.S. Government Printing Office): 307–317.

Bukry, D. & Bramlette M.N. 1969. Some new and stratigraphically useful calcareous nannofossils of the Cenozoic. *Tulane Studies in Geoloxy and Paleontology,* **7**: 131–142.

Bukry, D. & Percival, S.F. 1971. New Tertiary calcareous nannofossils. *Tulane Studies in Geology and Paleontology,* **8**: 123–146.

de Kaenel, E., Bergen, J., Browning, E., Blair, S., & Boesiger, T. 2017. Uppermost Oligocene to Middle Miocene *Discoaster* and *Catinaster* taxonomy and biostratigraphy in the circum North Atlantic Basin: Gulf of Mexico and ODP Leg 154. *Journal of Nannoplankton Research*, **37**(2/3), 215–244.

Gartner, S. Jr. 1969. Correlation of Neogene planktonic foraminifer and calcareous nannofossil zones. *Gulf Coast Association of Geological Societies. Transactions,* **19**: 585–599.

Gartner, S. & Bukry, D. 1974. *Ceratolithus acutus* Gartner and Bukry, n. sp. and *Ceratolithus amplificus* Bukry and Percival – nomenclatural clarification. *Tulane Studies in Geology and Paleontology,* **11**: 115–118.

Gartner, S. & Bukry, D. 1975. Morphology and Phylogeny of the Coccolithophycean Family Ceratolithaceae. *Journal Research U.S. Geological Survey,* **3**(4): 451–467.

Hay, W.W., Mohler, H.P., Roth, P.H., Schmidt, R.R. & Boudreaux, J.E. 1967. Calcareous nanoplankton zonation of the Cenozoic of the Gulf Coast and Caribbean-Antillean area, and transoceanic correlation. *Transactions of the Gulf Coast Assoc. Geologic Society,* **17**: 428–480.

Knüttel, S., Russell, M. D. & Firth, J.V. 1989. Neogene calcareous nannofossils from ODP Leg 105: Implications for Pleistocene paleogeographic trends. *In*: S.P. Srivastava, M.A. Arthur, B. Clement *et al., Proceedings of the ODP., Scientific Results*, **105**: College Station, TX (Ocean Drilling Program): 245–262.

Martini, E. 1971. Standard Tertiary and Quaternary calcareous nannoplankton zonation. *In*: A. Farinacci (Ed.). *Proceedings*

of the Second Planktonic Conference Roma 1970. Edizioni Tecnoscienza, Rome, **2**: 739–785.

Müller, C. 1974. Calcareous nannoplankton, Leg 25 (western Indian Ocean). *In*: E.S.W. Simpson, R. Schlich *et al., Initial Reports of the DSDP*, **25**: Washington D.C. (U.S. Government Printing Office): 579–633.

Okada, H. & Bukry, D. 1980. Supplementary modification and introduction of code numbers to the low-latitude coccolith biostratigraphic zonation (Bukry, 1973; 1975). *Marine Micropaleontology,* **5**: 321–325.

Perch-Nielsen, K. 1977. Albian to Pleistocene calcareous nannofossils from the western South Atlantic. *In*: P.R. Supko, K. Perch-Nielsen *et al. Initial Reports of the DSDP*, **39**: Washington D.C. (U.S. Government Printing Office): 699–823.

Perch-Nielsen, K. 1985. Cenozoic calcareous nannofossils. *In*: H.M. Bolli, J.B Saunders & K. Perch-Nielsen (Eds). *Plankton Stratigraphy*. Cambridge (Cambridge Univ. Press), 427–554.

Raffi, I., Backman, J. & Rio, D. 1998. Evolutionary trends of tropical calcareous nannofossils in the late Neogene. *Marine Micropaleontology,* **35**(1–2): 17–41.

Theodoridis, S. 1984. Calcareous nannofossil biozonation of the Miocene and revision of the helicoliths and discoasters. *Utrecht Micropaleontological Bulletins,* **32**: 1–271.

Wei, W. 2003. Upper Miocene nannofossil biostratigraphy and taxonomy of Exxon Core CH30-43-2 from the Gulf of Mexico. *Journal of Nannoplankton Research*, **25**(1): 17–23.

Wise, S.W., Jr. & Wind, F.H. 1977. Mesozoic and Cenozoic calcareous nannofossils recovered by DSDP Leg 36 drilling on the Falkland Plateau, southwest Atlantic section of the Southern Ocean. *In*: P.F. Barker, I.W.D. Dalziel, *et al*. *Initial Reports of the DSDP*, **36**: Washington (U.S. Government Printing Office): 269–491.

Young, J.R., Bergen, J.A., Bown, P.R., Burnett, J.A., Fiorentino, A., Jordan, R.W., Kleijne, A., van Niel, B.E. *et al.* 1997. Guidelines for coccolith and calcareous nannofossil terminology. *Palaeontology*, **40**: 875–912.

Plate 1

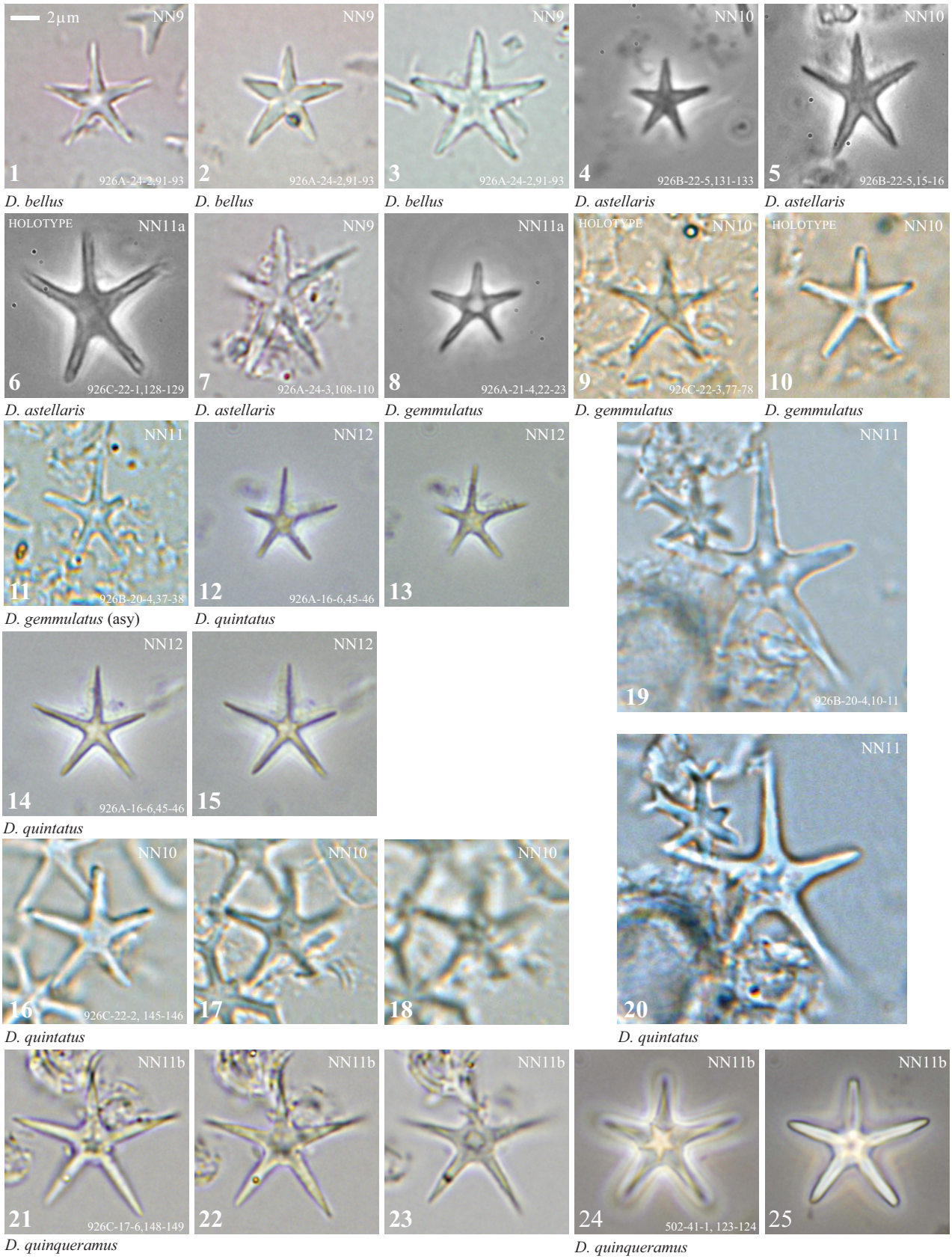
2µm
NN9
1
926A-24-2,91-93
D. bellus
NN9
2
926A-24-2,91-93
D. bellus
NN9
3
926A-24-2,91-93
D. bellus
NN10
4
926B-22-5,131-133
D. astellaris
NN10
5
926B-22-5,15-16
D. astellaris
HOLOTYPE
NN11a
6
926C-22-1,128-129
D. astellaris
NN9
7
926A-24-3,108-110
D. astellaris
NN11a
8
926A-21-4,22-23
D. gemmulatus
HOLOTYPE
NN10
9
926C-22-3,77-78
D. gemmulatus
HOLOTYPE
NN10
10
D. gemmulatus
NN11
11
926B-20-4,37-38
D. gemmulatus (asy)
NN12
12
926A-16-6,45-46
D. quintatus
NN12
13
NN11
19
926B-20-4,10-11
NN12
14
926A-16-6,45-46
D. quintatus
NN12
15
NN11
20
D. quintatus
NN10
16
926C-22-2, 145-146
D. quintatus
NN10
17
NN10
18
NN11b
21
926C-17-6,148-149
D. quinqueramus
NN11b
22
NN11b
23
NN11b
24
502-41-1, 123-124
D. quinqueramus
NN11b
25

Plate 2

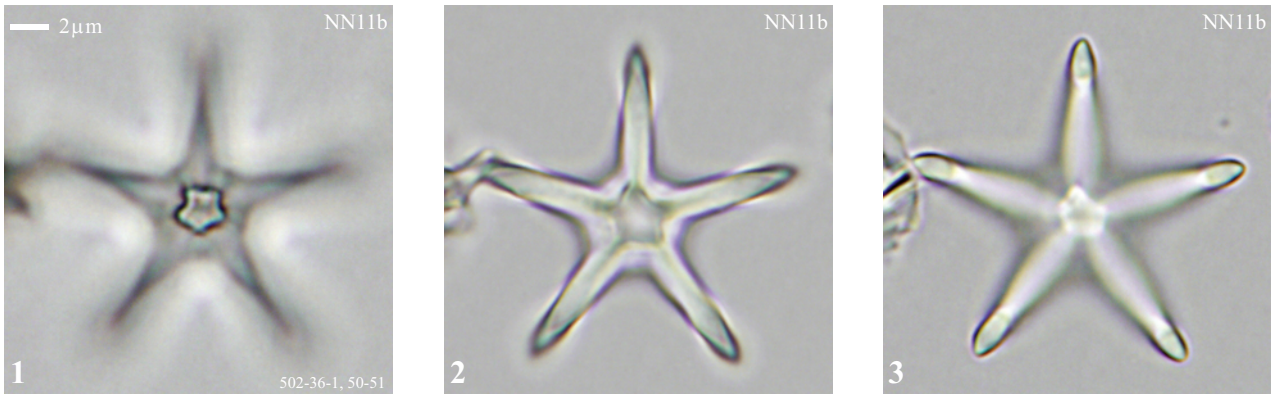

D. quinqueramus (>15)

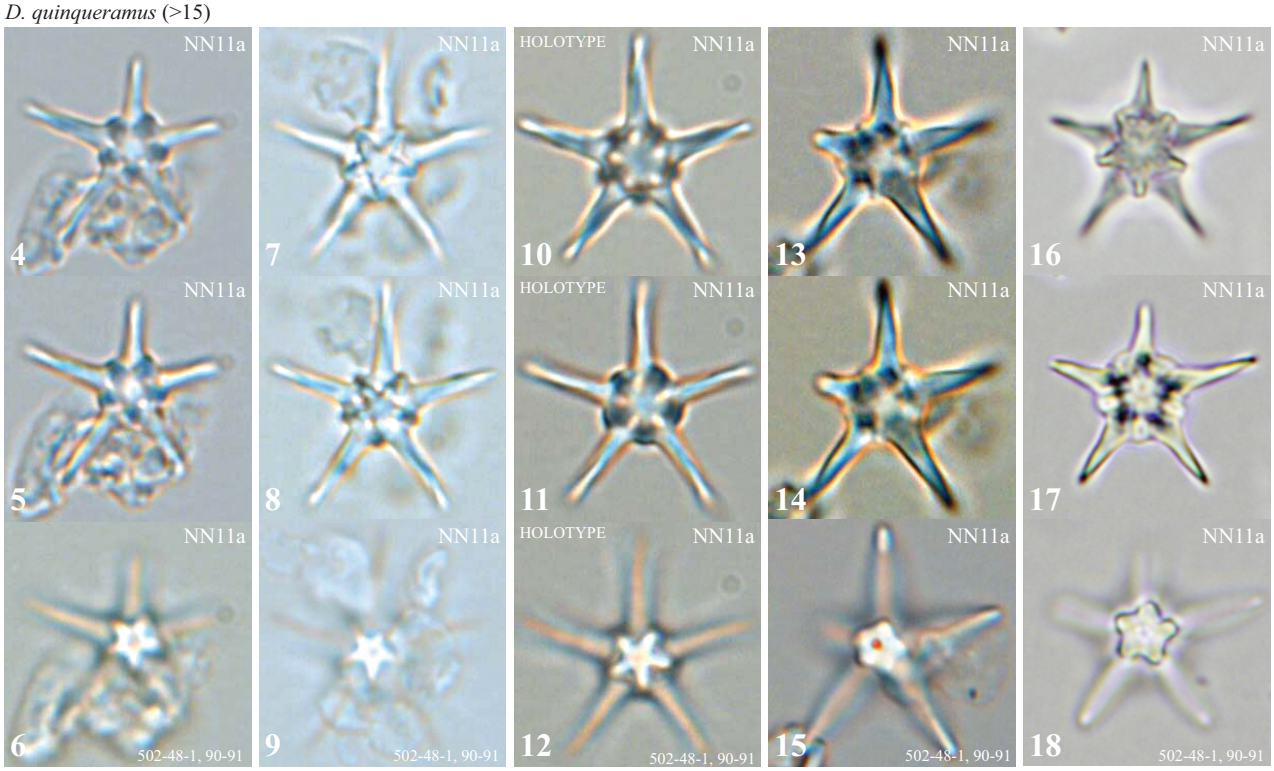

D. explicatus | *D. explicatus* | *D. explicatus* | *D. explicatus* | *D. explicatus* (trans)

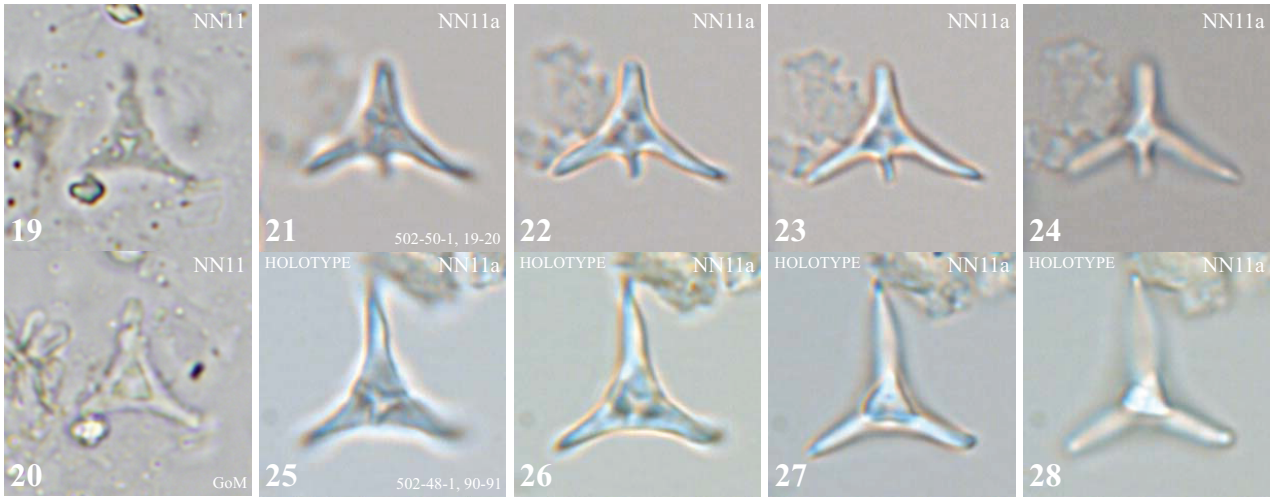

D. newellii | *D. newellii*

Plate 3

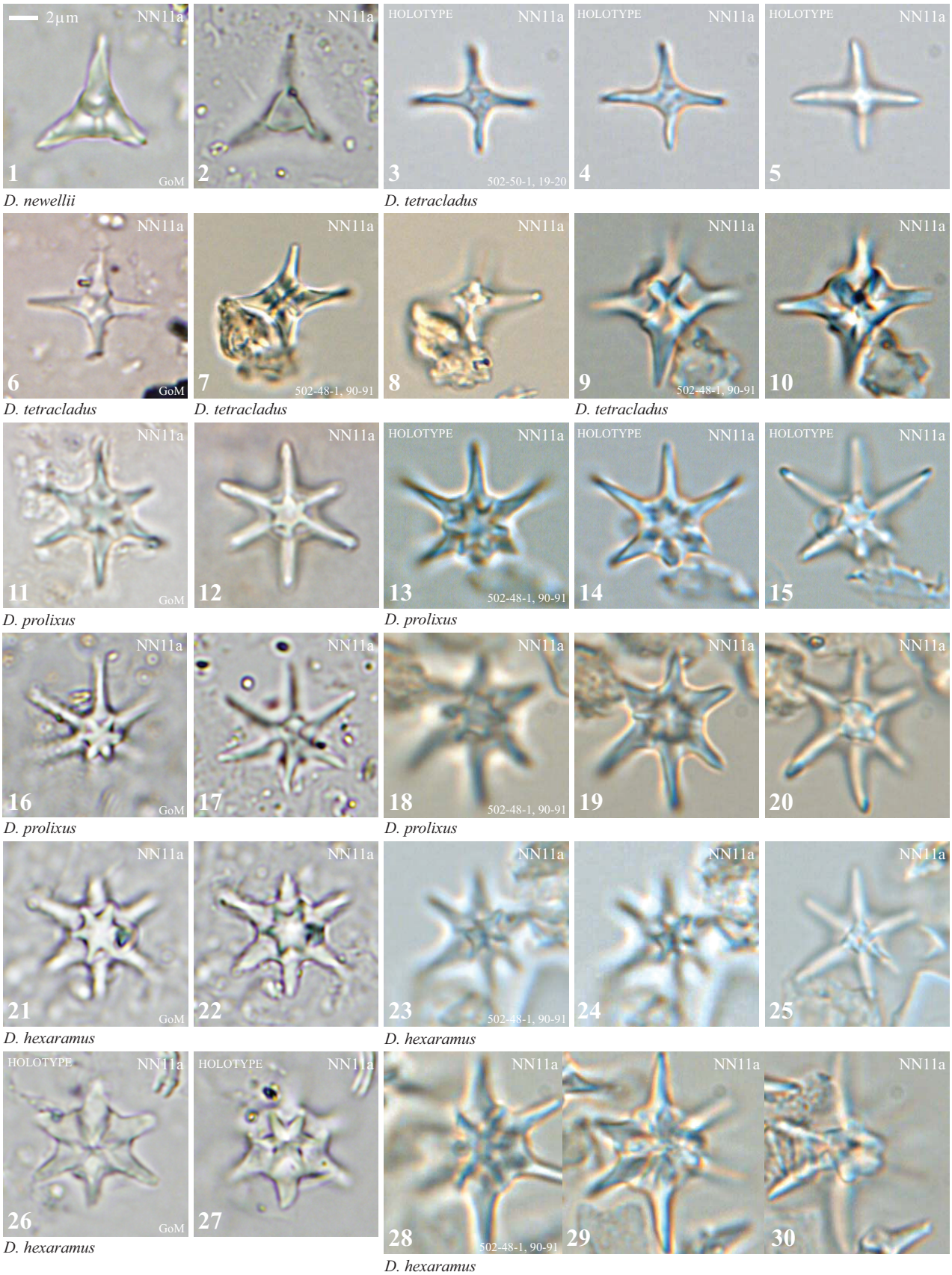
2µm
NN11a
1
GoM
2
HOLOTYPE
3
502-50-1, 19-20
4
5
D. newellii
D. tetracladus
6
7
502-48-1, 90-91
8
9
10
D. tetracladus
D. tetracladus
D. tetracladus
11
12
13
14
15
D. prolixus
D. prolixus
16
17
18
19
20
D. prolixus
D. prolixus
21
22
23
24
25
D. hexaramus
D. hexaramus
26
27
28
29
30
D. hexaramus
D. hexaramus

Plate 4

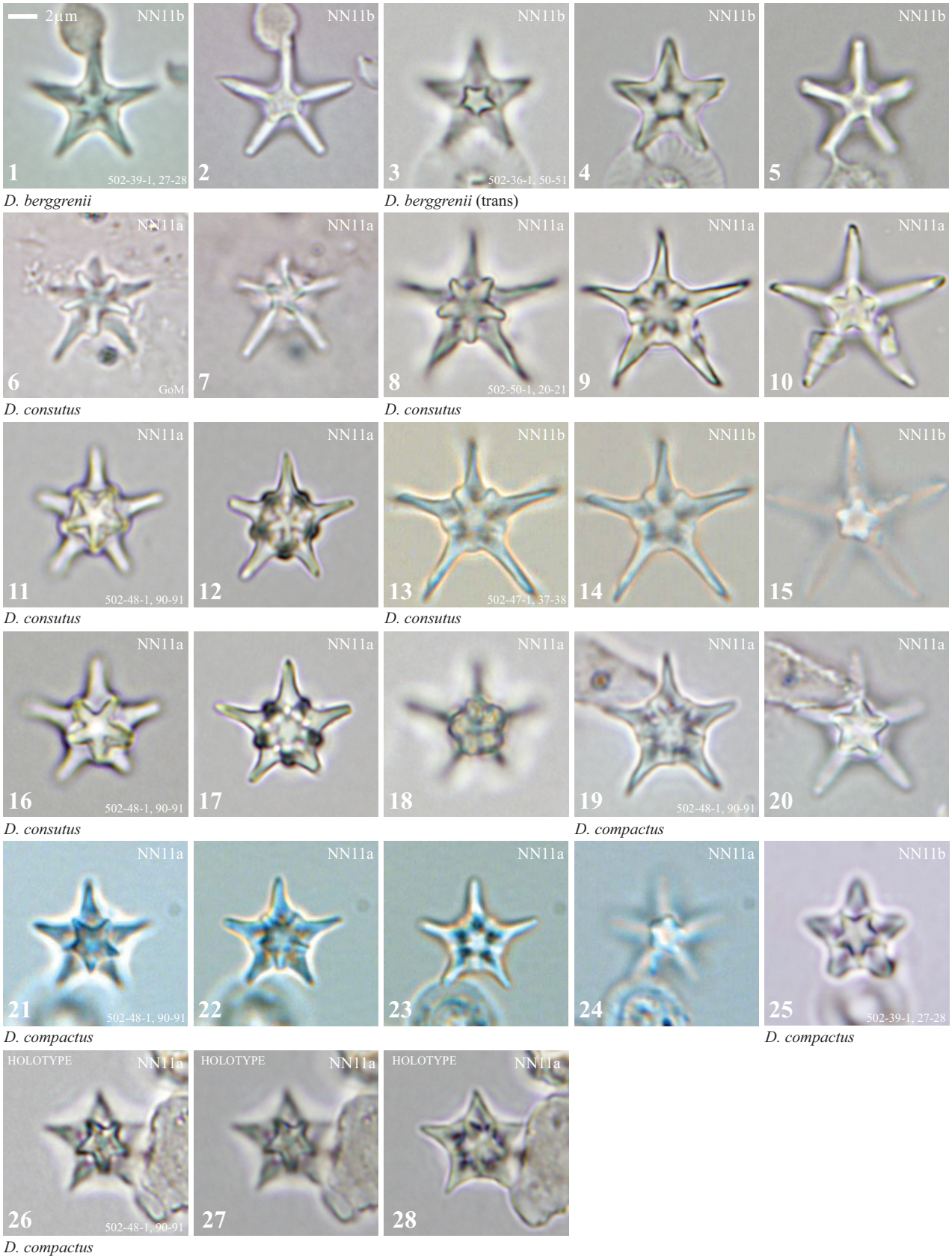
2µm
NN11b
1
502-39-1, 27-28
2
3
502-36-1, 50-51
4
5
D. berggrenii
D. berggrenii (trans)
NN11a
6
GoM
7
8
502-50-1, 20-21
9
10
D. consutus
D. consutus
11
502-48-1, 90-91
12
13
502-47-1, 37-38
14
15
D. consutus
D. consutus
16
502-48-1, 90-91
17
18
19
502-48-1, 90-91
20
D. consutus
D. compactus
21
502-48-1, 90-91
22
23
24
25
502-39-1, 27-28
D. compactus
D. compactus
HOLOTYPE
26
502-48-1, 90-91
27
28
D. compactus

Plate 5

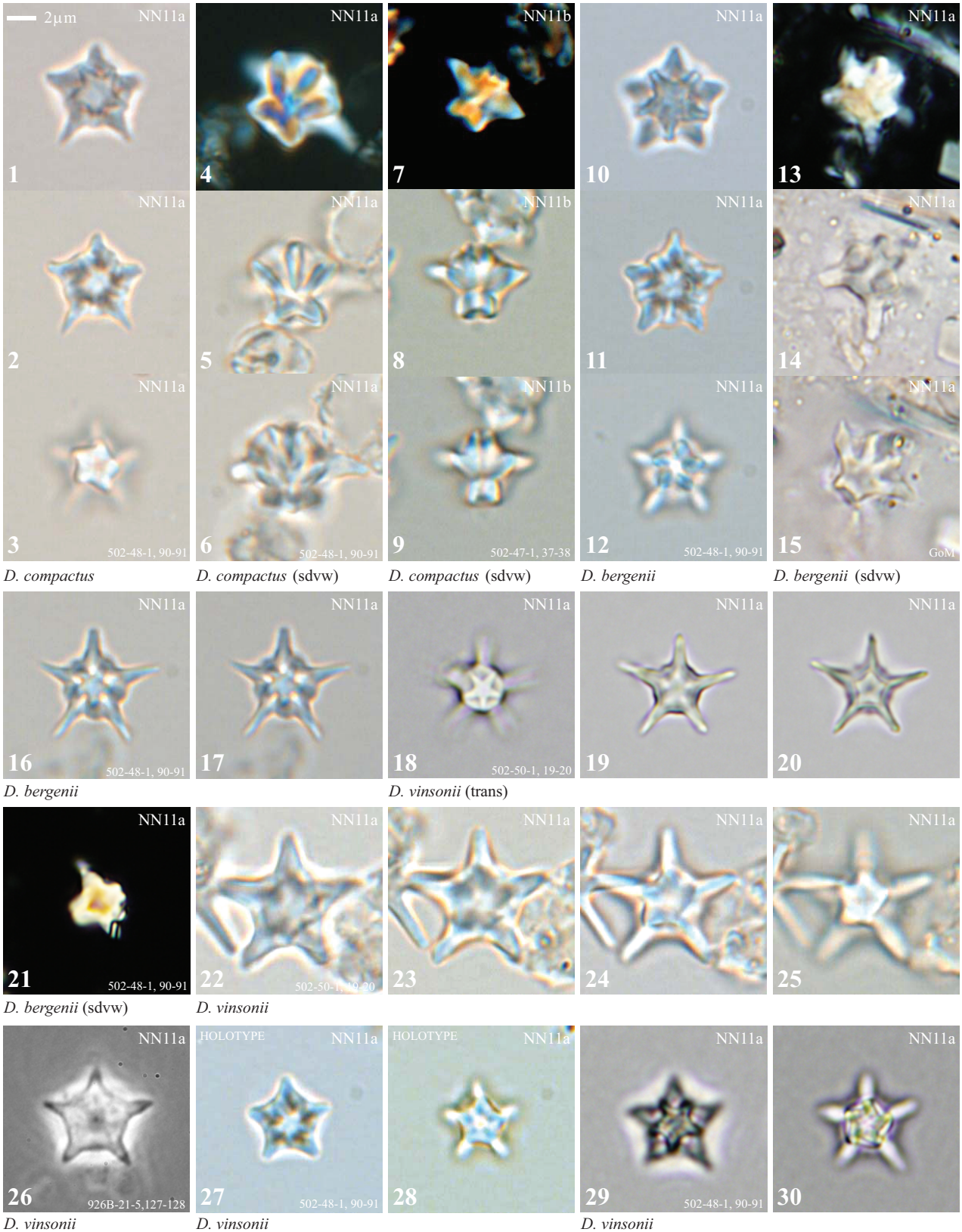
2µm
NN11a
1
NN11a
4
NN11b
7
NN11a
10
NN11a
13
NN11a
2
NN11a
5
NN11b
8
NN11a
11
NN11a
14
NN11a
3
502-48-1, 90-91
NN11a
6
502-48-1, 90-91
NN11b
9
502-47-1, 37-38
NN11a
12
502-48-1, 90-91
NN11a
15
GoM
D. compactus
D. compactus (sdvw)
D. compactus (sdvw)
D. bergenii
D. bergenii (sdvw)
NN11a
16
502-48-1, 90-91
NN11a
17
NN11a
18
502-50-1, 19-20
NN11a
19
NN11a
20
D. bergenii
D. vinsonii (trans)
NN11a
21
502-48-1, 90-91
NN11a
22
502-50-1, 19-20
NN11a
23
NN11a
24
NN11a
25
D. bergenii (sdvw)
D. vinsonii
NN11a
26
926B-21-5,127-128
HOLOTYPE
NN11a
27
502-48-1, 90-91
HOLOTYPE
NN11a
28
NN11a
29
502-48-1, 90-91
NN11a
30
D. vinsonii
D. vinsonii
D. vinsonii

Plate 6

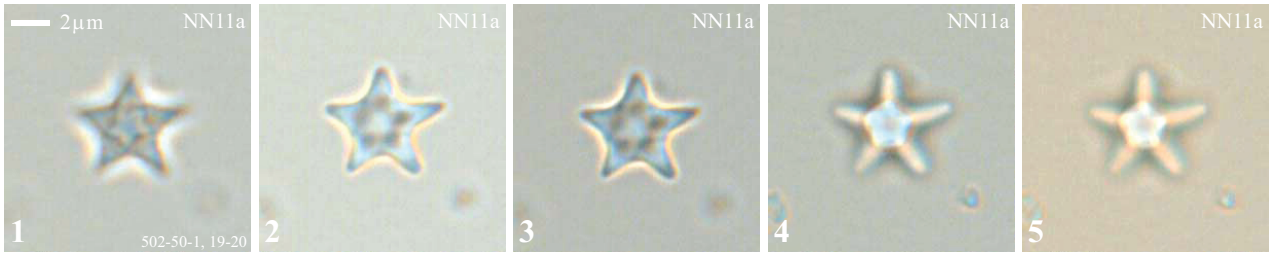

D. vinsonii

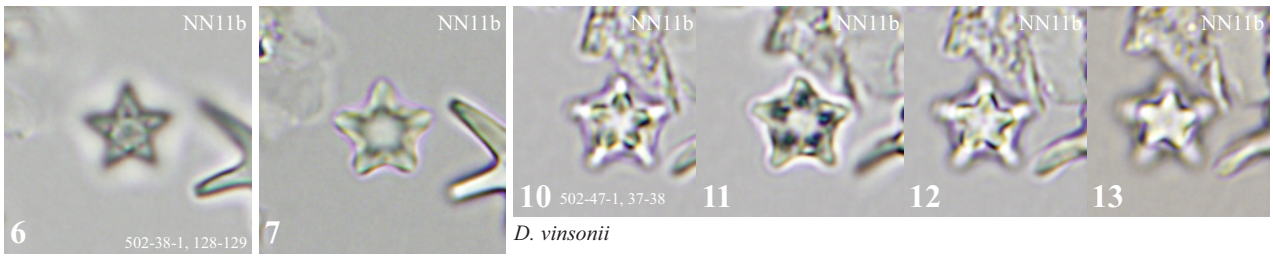

D. vinsonii *D. vinsonii*

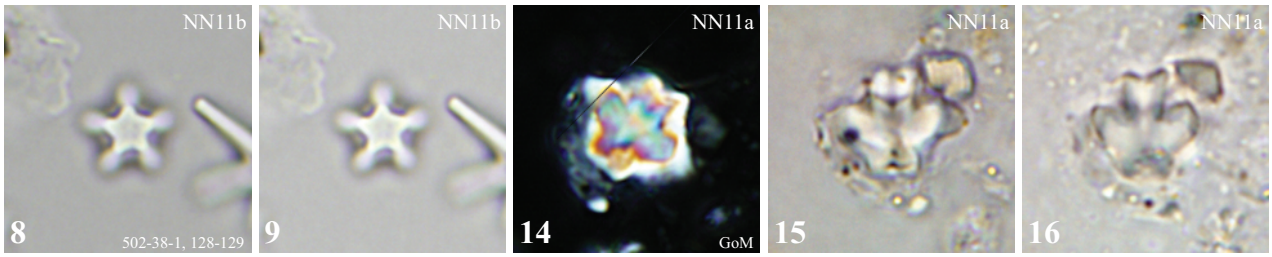

D. vinsonii *D. abrachiatus* (trans)

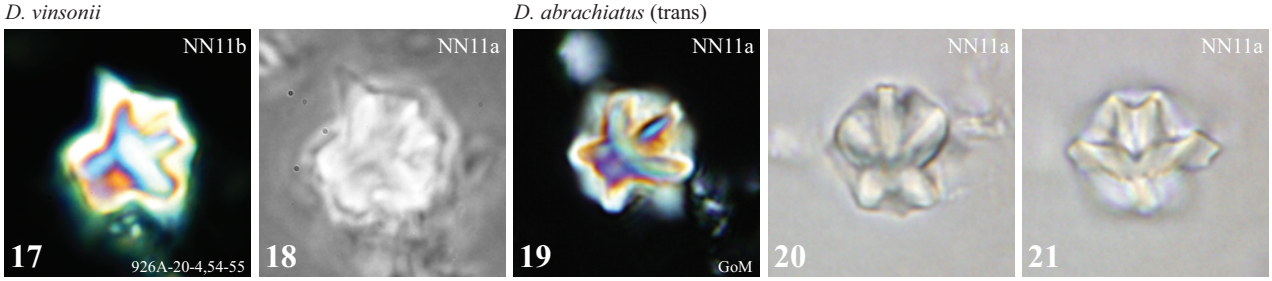

D. abrachiatus (trans) *D. abrachiatus*

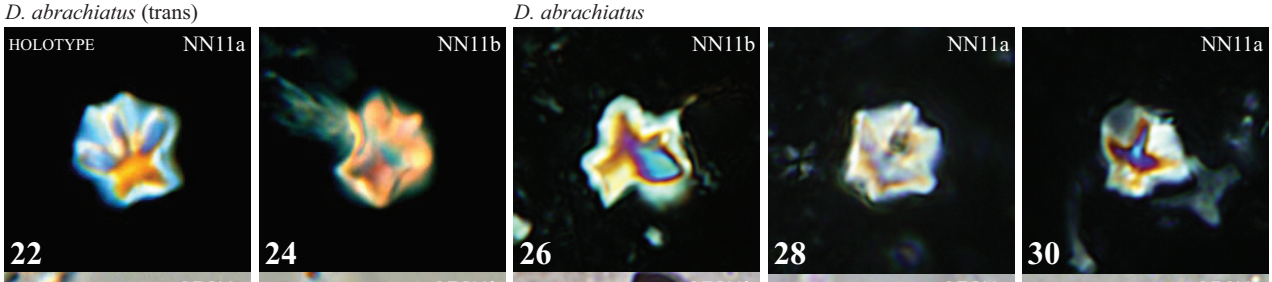

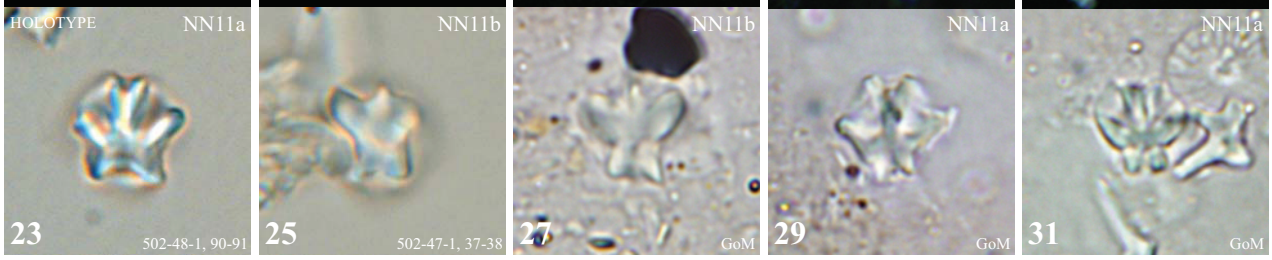

D. abrachiatus *D. abrachiatus* *D. abrachiatus* *D. abrachiatus* *D. abrachiatus*

Plate 7

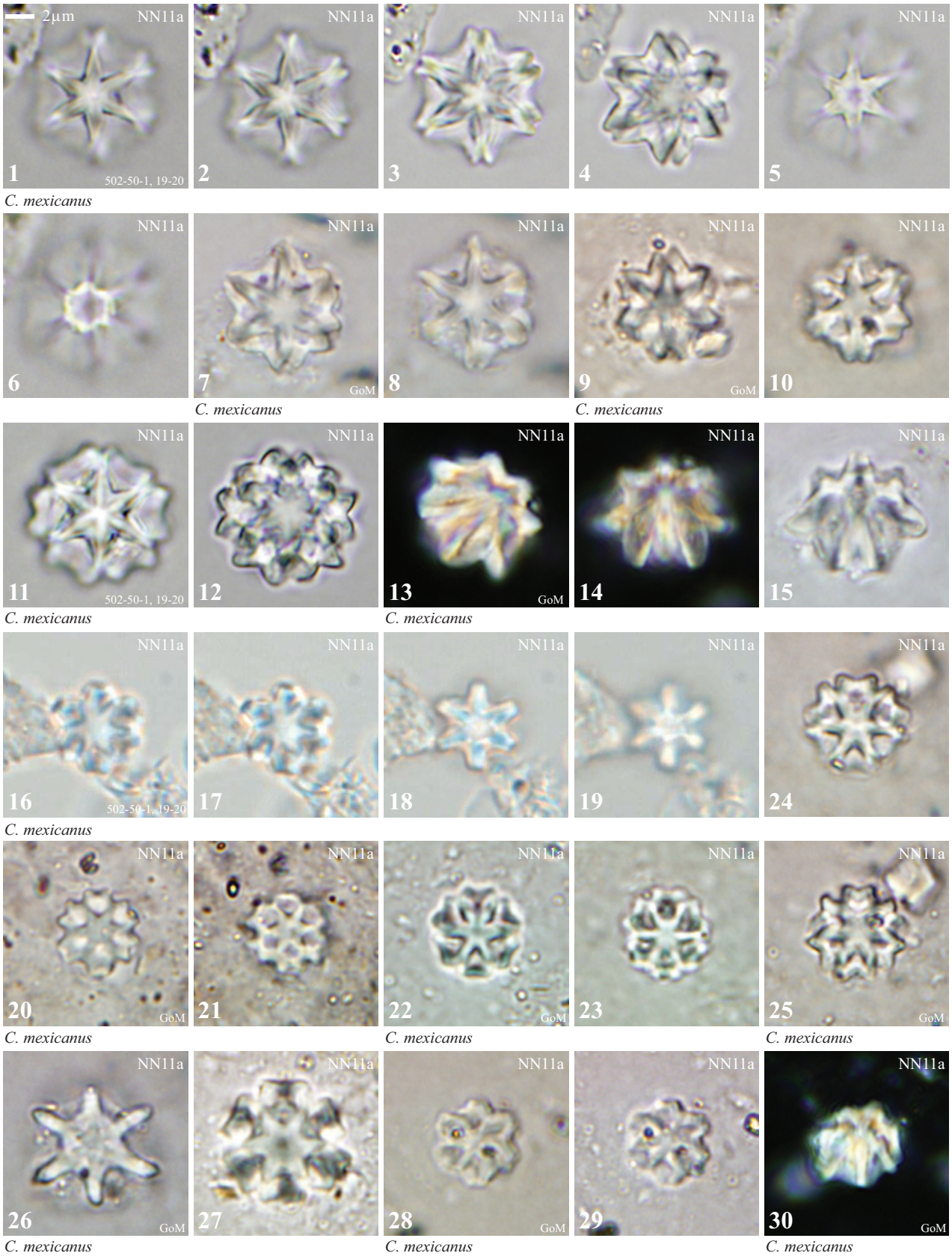
2µm
NN11a
1
502-50-1, 19-20
2
3
4
5
C. mexicanus
6
7
GoM
8
9
10
C. mexicanus
C. mexicanus
11
502-50-1, 19-20
12
13
GoM
14
15
C. mexicanus
C. mexicanus
16
502-50-1, 19-20
17
18
19
24
C. mexicanus
20
GoM
21
22
GoM
23
25
GoM
C. mexicanus
C. mexicanus
C. mexicanus
26
GoM
27
28
GoM
29
30
GoM
C. mexicanus
C. mexicanus
C. mexicanus

Plate 8

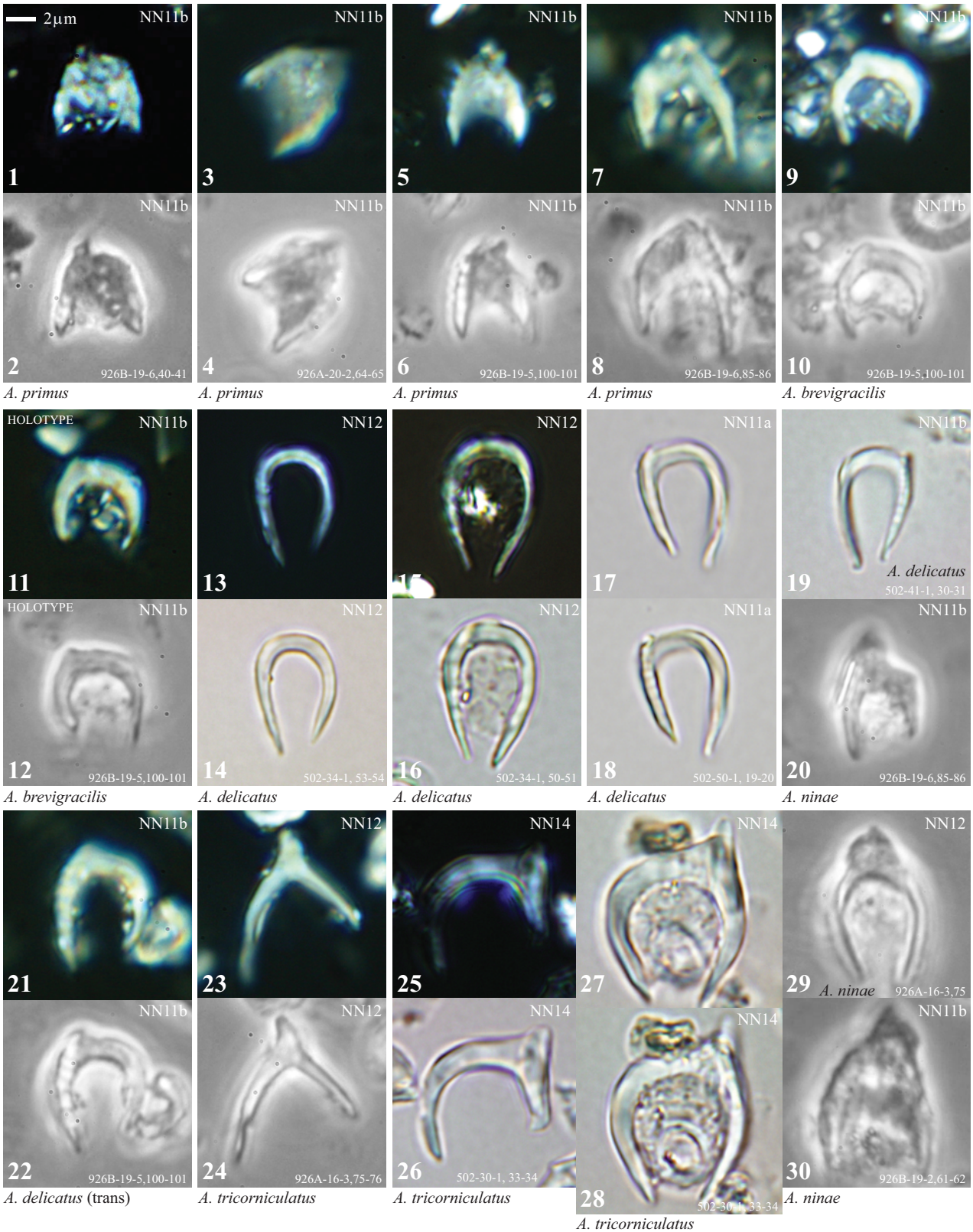
2µm
NN11b
1
3
5
7
9
2
926B-19-6,40-41
4
926A-20-2,64-65
6
926B-19-5,100-101
8
926B-19-6,85-86
10
926B-19-5,100-101
A. primus
A. primus
A. primus
A. primus
A. brevigracilis
HOLOTYPE
11
NN12
13
15
NN11a
17
19
A. delicatus
502-41-1, 30-31
12
926B-19-5,100-101
14
502-34-1, 53-54
16
502-34-1, 50-51
18
502-50-1, 19-20
20
926B-19-6,85-86
A. brevigracilis
A. delicatus
A. delicatus
A. delicatus
A. ninae
NN14
21
23
25
27
29
A. ninae
926A-16-3,75
22
926B-19-5,100-101
24
926A-16-3,75-76
26
502-30-1, 33-34
28
30
926B-19-2,61-62
A. delicatus (trans)
A. tricorniculatus
A. tricorniculatus
A. tricorniculatus
A. ninae

Plate 9

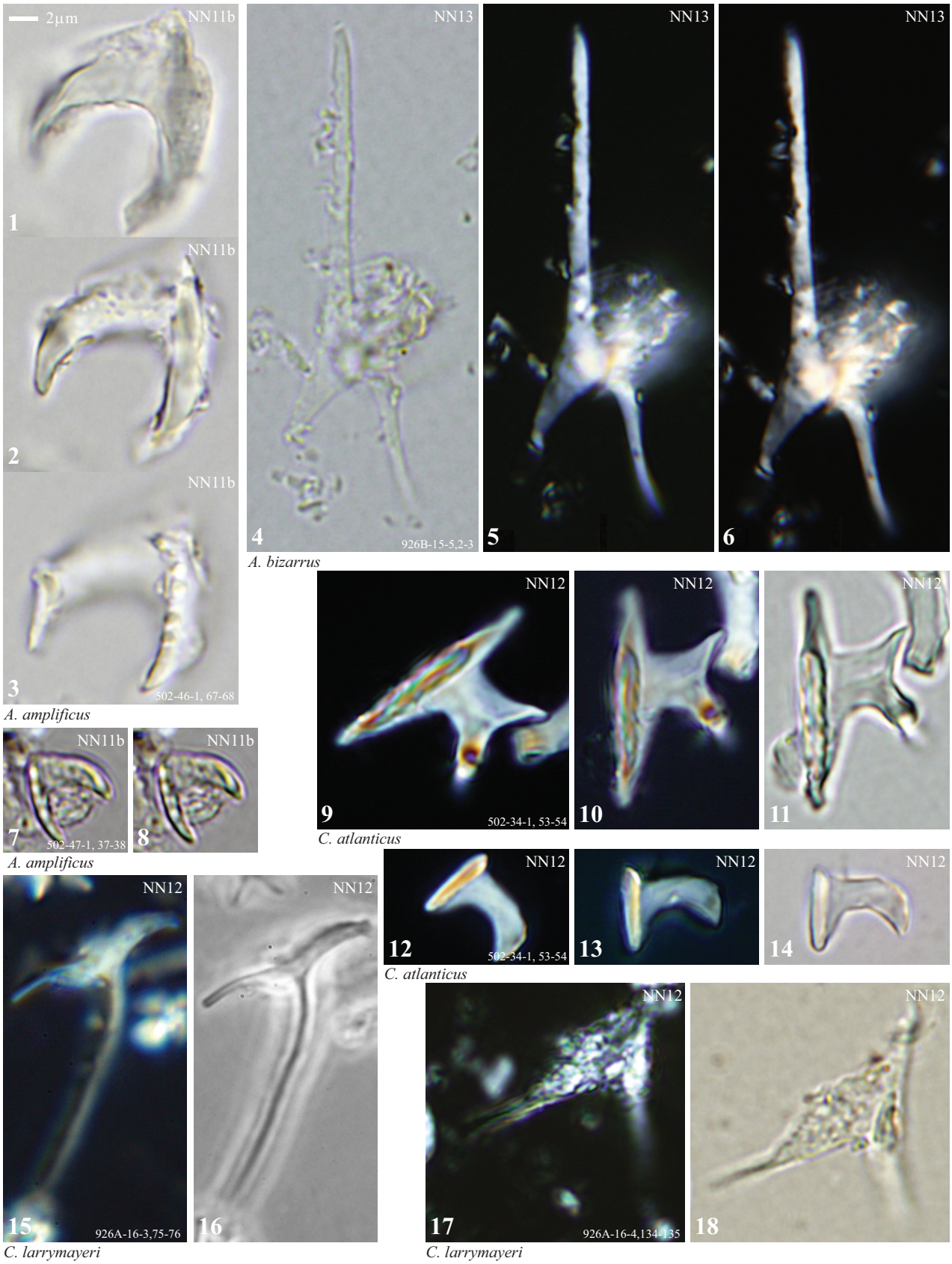
2µm
NN11b
1
NN11b
2
NN11b
3
502-46-1, 67-68
A. amplificus
NN13
4
926B-15-5,2-3
A. bizarrus
NN13
5
NN13
6
NN12
9
502-34-1, 53-54
NN12
10
NN12
11
C. atlanticus
NN11b
7
502-47-1, 37-38
NN11b
8
A. amplificus
NN12
12
502-34-1, 53-54
NN12
13
NN12
14
C. atlanticus
NN12
15
926A-16-3,75-76
NN12
16
C. larrymayeri
NN12
17
926A-16-4,134-135
NN12
18
C. larrymayeri

Plate 10

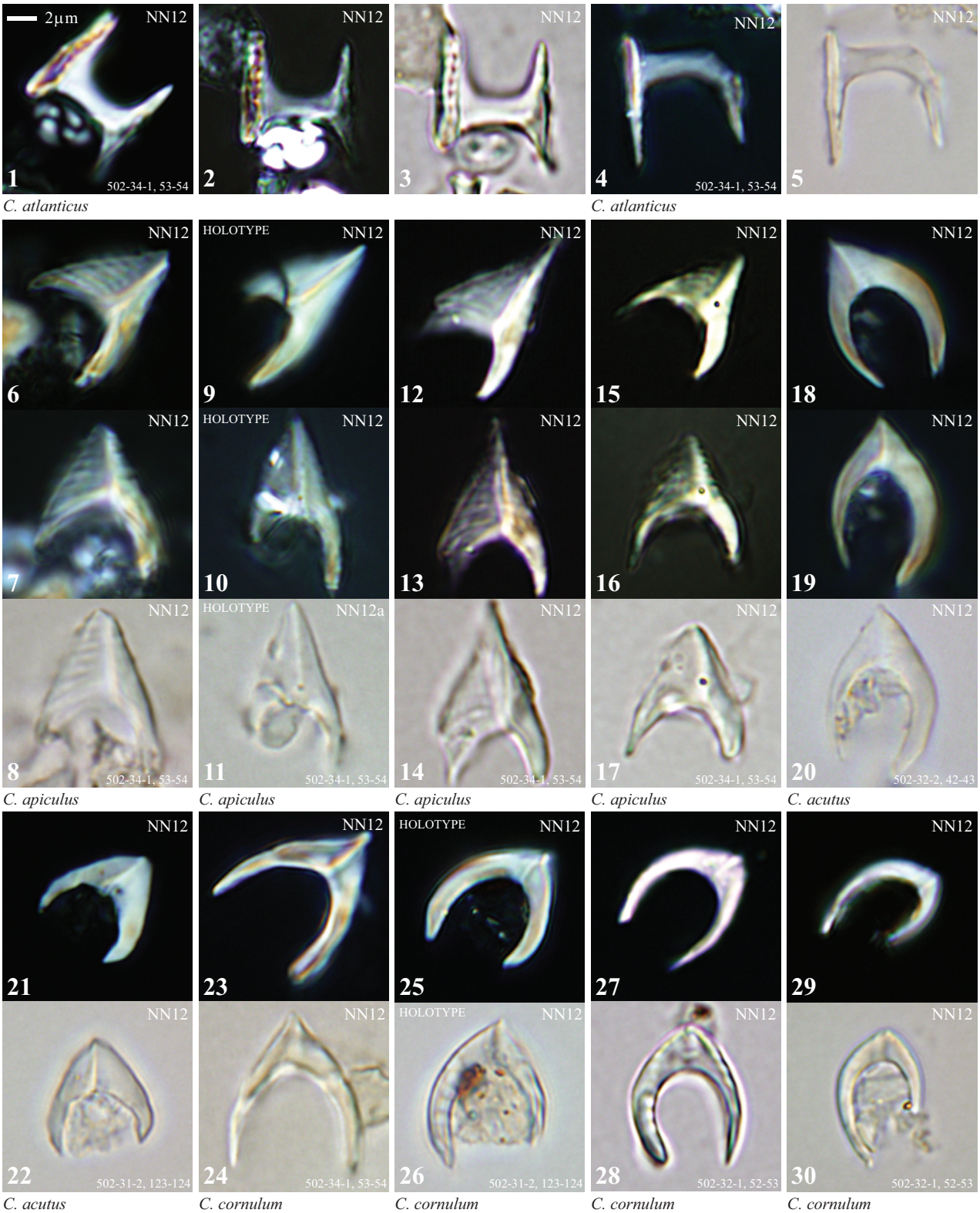
2µm
NN12
1
502-34-1, 53-54
2
3
4
502-34-1, 53-54
5
C. atlanticus
C. atlanticus
6
7
HOLOTYPE
9
10
12
13
15
16
18
19
8
502-34-1, 53-54
HOLOTYPE
NN12a
11
502-34-1, 53-54
14
502-34-1, 53-54
17
502-34-1, 53-54
20
502-32-2, 42-43
C. apiculus
C. apiculus
C. apiculus
C. apiculus
C. acutus
21
23
HOLOTYPE
25
27
29
22
502-31-2, 123-124
24
502-34-1, 53-54
26
502-31-2, 123-124
28
502-32-1, 52-53
30
502-32-1, 52-53
C. acutus
C. cornulum
C. cornulum
C. cornulum
C. cornulum

Plate 11

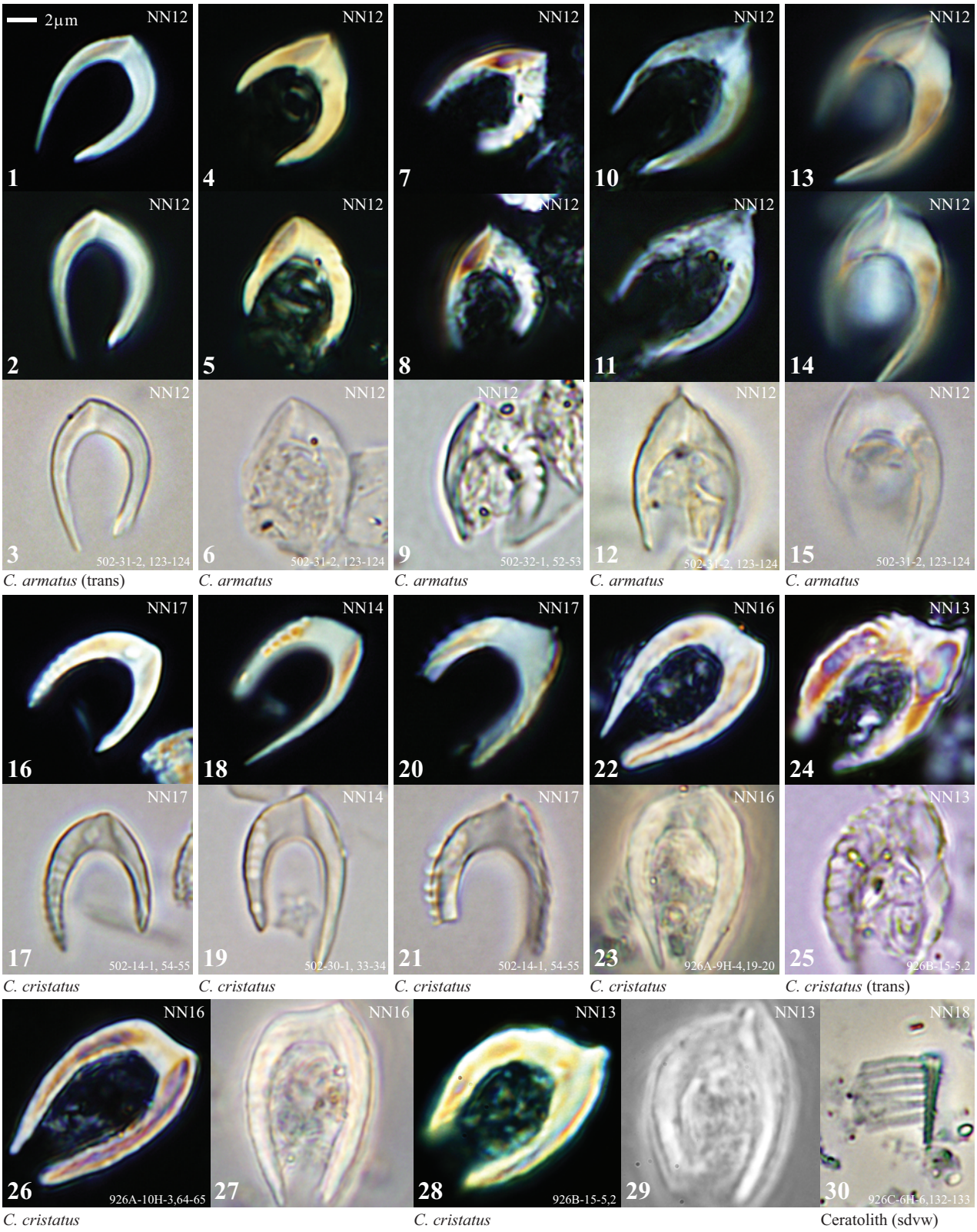

C. armatus (trans) | *C. armatus* | *C. armatus* | *C. armatus* | *C. armatus*

C. cristatus | *C. cristatus* | *C. cristatus* | *C. cristatus* | *C. cristatus* (trans)

C. cristatus | *C. cristatus* | Ceratolith (sdvw)

Plate 12

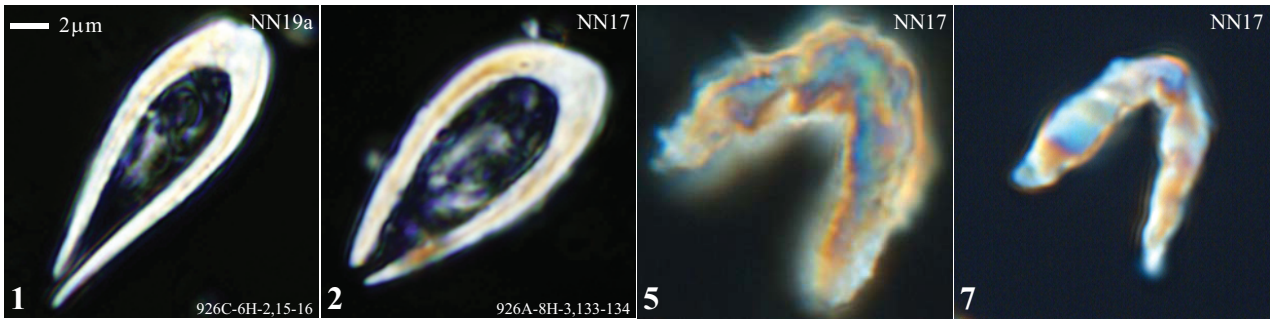

C. telesmus *C. telesmus*

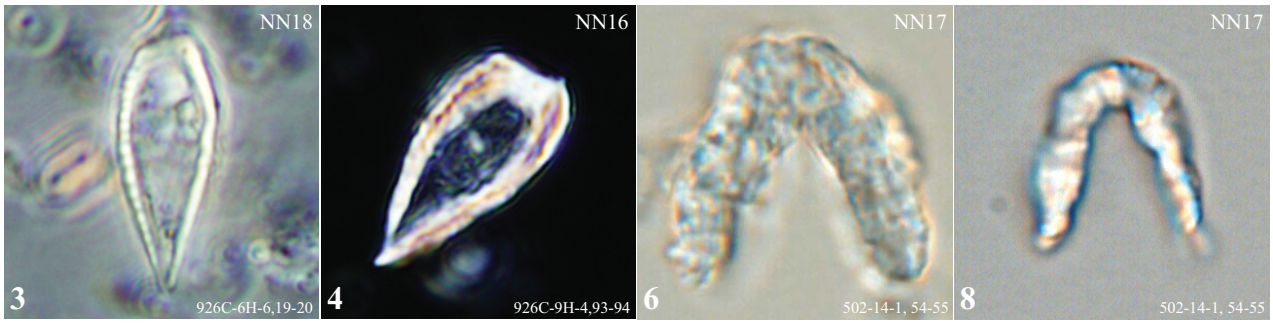

C. telesmus *C. telesmus* *C. rugosus* *C. rugosus*

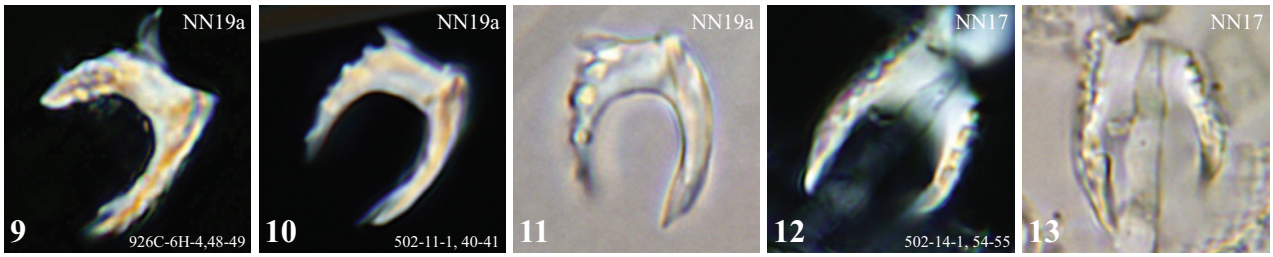

C. separatus *C. separatus* *C. separatus*

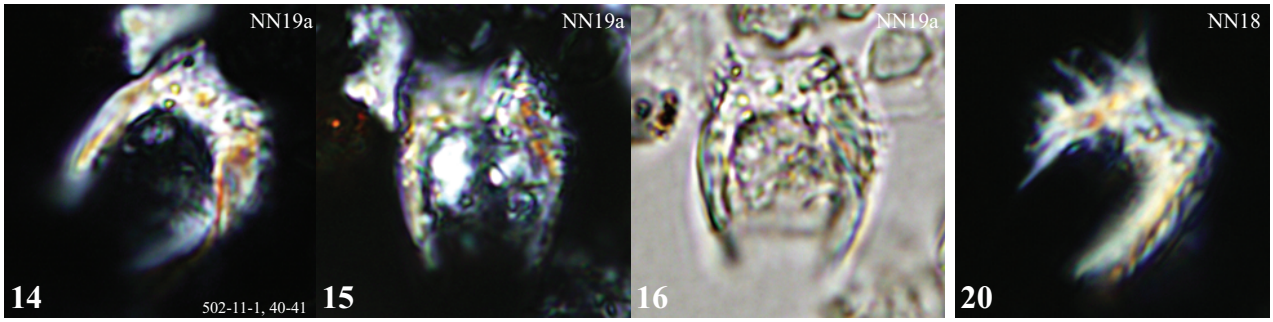

C. separatus

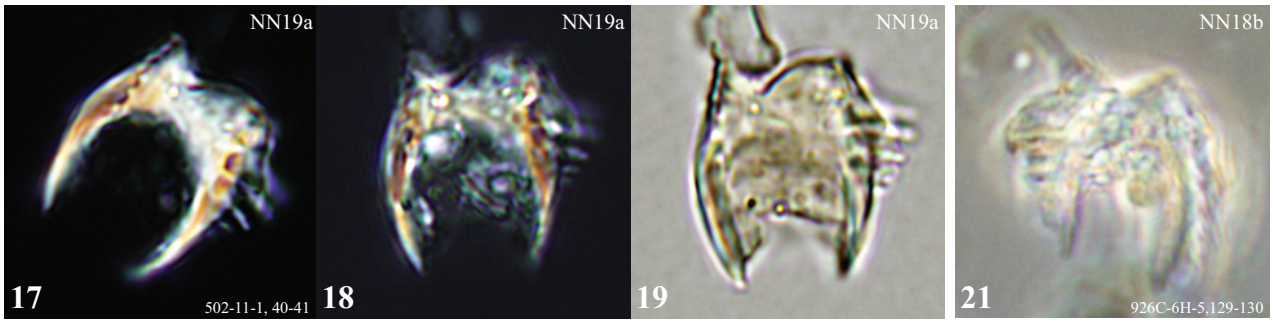

C. separatus *C. separatus*